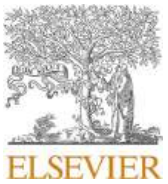
International Journal of Disaster Risk Reduction 146 (2026) 106473



Contents lists available at ScienceDirect

International Journal of Disaster Risk Reduction

journal homepage: www.elsevier.com/locate/ijdrr



A decision-support tool for fire risk assessment and mitigation of motorway bridges: A European case study

Patrick Covi [a,*], Marco Guerrieri [a], Nicola Tondini [a]

[a] Department of Civil, Environmental and Mechanical Engineering, University of Trento, Via Mesiano 77, Trento, 38123, Italy

ARTICLE INFO

Keywords:
Fire accident risk
Bridges
HSM manual
Motorway
Trans European road network

ABSTRACT

Fires represent a significant threat to civil infrastructures and structures, including bridges. Bridge fire events are typically triggered by the presence of flammable materials, most commonly involving vehicle accidents or the transport of combustible goods. Despite a lower probability of occurrence than for buildings, the consequences can be high: bridge structural integrity can be severely compromised, potentially leading to substantial economic losses due to repair costs, traffic disruption, and loss of serviceability. In recent years, the frequency and impact of fire incidents affecting transportation infrastructure have increased, highlighting the vulnerability of bridges to such extreme events. However, current bridge design standards and regulations do not provide fire design criteria, resulting in a critical gap in infrastructure resilience assessment. This study aims to develop a risk-based model for assessing fire hazards in highway bridges, intended as a practical decision-support tool for infrastructure managers to identify critical scenarios and prioritise mitigation strategies. The proposed framework integrates key factors, including traffic composition, structural typology, damage scenarios, and their associated direct and indirect consequences. The model is designed to be applicable at the network level, enabling a systematic evaluation of bridge fire vulnerability. The methodology is applied to a real-world case study of a motorway within the Trans-European Transport Corridor, characterised by high volumes of heavy-vehicle traffic and of strategic economic and social importance. Results demonstrate the effectiveness of the proposed approach in capturing fire-risk variability across different bridge configurations and traffic conditions, providing valuable insights for risk-informed decision-making and targeted risk mitigation measures.

1. Introduction

Bridges are strategic infrastructures designed to withstand operating and exceptional load conditions. However, fire poses a substantial risk to bridge structures, which are generally designed without specific fire-resistance criteria. In fact, unlike other structures such as buildings and tunnels, bridge designers lack specific regulatory standards for evaluating fire resistance. This is due to the fact that fire safety concepts have been mainly developed for life safety, which can be highly endangered by compartment fires in buildings, whereas fires involving bridges are not generally life-threatening, but can highly affect the functionality of the infrastructural network with long disruptions and high costs. Thus, it is essential to assess structural deformations and evaluate the associated collapse risk. Excessive deformations not only compromise bridge functionality, leading to severe disruptions, but may also

* Corresponding author.
E-mail addresses: patrick.covi@unitn.it (P. Covi), marco.guerrieri@unitn.it (M. Guerrieri), nicola.tondini@unitn.it (N. Tondini).

https://doi.org/10.1016/j.ijdrr.2026.106473
Received 10 July 2026; Received in revised form 3 October 2026; Accepted 3 October 2026
Available online 5 October 2026
2212-4209/© 2026 The Authors. Published by Elsevier Ltd. This is an open access article under the CC BY-NC-ND license (http://creativecommons.org/licenses/by-nc-nd/4.0/).

damage utility systems and underground services incorporated into the structure, with potentially far-reaching consequences. Examples of such fire events include the I-95 Overpass Collapses in Philadelphia (June 11, 2023) and the A21 Overpass in Italy (January 2, 2018). Several research works have reported past bridge fire accidents, especially in the United States [1,2].

In the United States alone, the estimated average annual losses from fire-damaged bridges amounted to $1.28 billion in 2002 [2]. The primary causes of fire ignition can be categorised as fires triggered by vehicle defects or vehicle collisions. Fires following collisions can be exceptionally intense, often due to the rapid ignition of highly flammable materials. Fires resulting from vehicle defects typically start with the engine, exhaust system, wheels, or brakes, and rarely in the cargo. Such fires typically develop slowly at first but may intensify over time, allowing for early extinguishment or containment using portable fire extinguishers or fire brigade intervention. Post-collision fires are often accelerated by fuel leakage, resulting in significantly faster development. Flammable liquid fires, such as pool fires involving large amounts of flammable liquids, are rare events that require significant liquid release, typically following a collision or another major incident.

Bridges with steel girders or cables/stays, as well as steel-concrete composite structures, are particularly vulnerable due to the exposed unprotected steelwork. The load-bearing capacity of these structures diminishes quickly due to the rapid heating of steel elements during a fire, and they are often designed with statically determined schemes that lack robustness in fire scenarios. This may also apply to prestressed concrete bridges for which the use of high-strength concrete allows for the reduction of the size of the cross sections, but its low porosity can enhance spalling and damage. Moreover, the effect of fire on the prestressing tendons can lead to a large extent of prestressing loss, undermining the bridge safety, as for the A21 Overpass in Italy [3–5], which was demolished and rebuilt as a fire-protected steel solution. Moreover, the closure of a bridge can have significant economic repercussions on the infrastructural network. The recent bridge collapses in Italy have highlighted the major disruptions they can cause to the operation of nearby road networks and the prolonged, indirect economic losses they can entail. For example, the collapse of the Morandi bridge (Polcevera bridge) resulted in immediate indirect losses of 359.1 m€, with estimated annual losses to the Italian economy approaching 1 bn€ [2].

Recently, there has been increased focus on investigating the structural behaviour of bridges under fire scenarios. Researchers analysed bridge failure causes [1,2,6–9], performed numerical simulations [10–15] and conducted experimental tests [16,17]. Fire hazards affecting bridges and transportation infrastructure have also been reviewed and assessed [1,18], while the fire vulnerability of two bridge typologies relevant to the present research was analysed in Ref. [19,20]. Beyond the structural consequences of bridge damage, the disruption of bridge infrastructure and its associated indirect economic impacts have also been investigated [21].

The growth in traffic demand causes several problems both in urban and extra-urban road networks, including the deterioration of levels of service (LOS), oversaturation conditions, queue formation, increased pollutant emissions, and insufficient safety conditions. In 2021, an estimated 1.19 million people died in road traffic crashes [22], and road traffic safety remains a serious public health concern worldwide. In the EU27 as a whole, there were 20,385 deaths in road accidents during 2023, with 45 road deaths every million inhabitants. In the same year, in Italy there were 3039 deaths in road accidents, 224,634 injuries, and 166,525 road accidents [23].

Over the past decades, numerous studies have examined accident causation and risk factors. The literature highlights that factors such as high speed, distracted and aggressive driving, non-compliance with traffic rules and signs, traffic flow intensity, horizontal and vertical road alignment, and intersection layouts are among the most prevalent factors affecting road safety [24,25]. The detection of hazardous road segments may help identify appropriate countermeasures to improve safety and optimise maintenance budget and resources [24].

One of the most useful and widely recognized methods for evaluating accidents and risk factors in highway engineering is represented by the Highway Safety Manual - HSM [26] which includes statistically derived regression models, commonly called safety performance functions (SPFs), that allow the estimation of the expected number of crashes along different road and highway facilities (rural two-lanes two-way, highways, urban arterials, suburban arterials, rural multilane and highways).

SPFs permit the correlation of the expected mean annual crash frequency with selected geometric parameters and traffic volumes of a highway. Since SPFs were developed from data collected at selected sites in the United States, they are defined under specific base conditions in terms of road alignment, cross-section geometry, traffic volumes, and traffic rules. The key elements of the HSM predictive method are therefore “base” SPFs, which estimate the average crash frequency under a defined set of “base conditions” for each road or facility type [27].

Every time one or more parameters of the specific road, intersection or facility under study deviate from the base conditions detailed in the HSM, the “base” crash frequencies calculated with the SPFs should be adjusted using specific Crash Modification Factors (CMFs). These modifications are necessary to adapt the results of SPFs to non-base conditions for a given case study (e.g., lane and median width, shoulder type and width, lighting conditions, enforcement, etc.). To apply the HSM procedure to other countries, it is necessary to adjust SPF crash estimates using specific crash modification factors (CMFs) [28]. This step is essential because crash frequencies may vary considerably across jurisdictions due to factors such as climate, driver behaviour, animal populations, crash reporting thresholds, and local reporting procedures [26]. Finally, HSM presents some general procedures for the issue of calibration versus modelling [29] and suggests developing calibration factors considering 30-50 randomly selected sites with at least 100 crashes per year [29].

On these premises, the aim of this research is to propose a decision-support methodology that can support Bridge Management Systems in identifying and prioritising economically sustainable actions to mitigate fire risk for highway bridges. To this end, the method integrates properly calibrated accident prediction models, accounts for potential structural damage resulting from vehicle fire events, and incorporates implementation costs of mitigation measures.

The proposed methodology has been applied to one of the most trafficked European motorways, serving as a representative and demanding case study. However, the article does not provide specific information on the road infrastructure analysed due to privacy

restrictions imposed by the motorway operator.

In summary, the main novelty of this research lies in the integration of accident prediction models commonly employed in road and traffic engineering with methodological approaches traditionally adopted in the structural engineering of large-scale infrastructure, particularly bridges.

The remainder of the article is organised as follows. Section 2 describes the research methodology, including the HSM-based accident prediction framework and calibration procedure. Section 3 presents the main characteristics of the analysed motorway and the data collection process. Section 4 reports the results of the traffic and accident analyses. Section 5 details the fire risk assessment, including probability estimation, consequence analysis, and cost calculations based on the fire vulnerability analyses of common bridge typologies. Finally, the conclusions of this study were reported.

2. Research methodology

The proposed methodology adopts a risk-based, multi-scale framework that links traffic safety, fire-event occurrence, structural vulnerability, and network-level consequences within a unified decision-support process. The underlying principle is to propagate the effects of a potential vehicle-related fire from its initiating event to the resulting structural and operational consequences, while maintaining consistency between the probabilistic description of the hazard and the deterministic assessment of structural response. The framework is therefore conceived as a sequential but interconnected chain of analyses, in which traffic level, composition, in terms of light and heavy vehicles percentages, and infrastructure characteristics define the exposure, accident models quantify the likelihood of fire-initiating events, structural analyses characterise the resulting damage states, and traffic and cost models translate infrastructure damage into network-level consequences. This integrated structure represents the main methodological contribution of the study, combining approaches traditionally developed independently in highway safety engineering and structural fire engineering.

At the traffic-engineering level, the motorway is discretised into homogeneous basic segments for which traffic demand, vehicle composition, geometric characteristics, and roadside features are defined. The expected crash frequency is estimated using the Highway Safety Manual (HSM) Safety Performance Functions (SPFs), subsequently modified through Crash Modification Factors (CMFs) and locally calibrated to account for the specific characteristics of the analysed motorway. The resulting segment-specific crash frequencies are then combined with the observed proportion of fire-producing events, with particular consideration of light- and heavy-vehicle involvement, to obtain the spatial distribution of the fire hazard. Future traffic demand is also incorporated to account for the evolution of exposure over the assessment horizon.

The structural component subsequently establishes the consequence side of the risk assessment. Representative bridge typologies and fire scenarios are considered to characterise the thermal exposure, structural temperature field, deformation response, loss of load-bearing capacity, and potential collapse or loss of functionality. The structural response is thereby translated into engineering-level damage and serviceability states that can be associated with each fire scenario. The probability of occurrence and the structural consequences are finally combined according to a risk formulation and extended to include the direct and indirect economic effects associated with bridge damage, traffic restrictions, and loss of network performance.

The resulting risk indicators are used within a Bridge Management System perspectve to rank vulnerable locations and assess the effectiveness and economic efficiency of alternative mitigation measures. In this way, the methodology moves from conventional component-level safety assessment towards a network-oriented risk management framework, in which the prioritisation of interventions is driven not only by the probability of a fire event or the structural damage itself, but also by the resulting degradation of motorway performance and associated user and infrastructure costs.

2.1. Fire accident frequency estimation

The Highway Safety Manual (HSM) represents a useful support tool for road operators. This procedure has been adapted and applied to fire accidents involving a bridge on a selected road and is founded on three main very different elements: the SPFs, which are the base-function and are related only to the main road segment characteristics; the CMFs that permit to consider the specific characteristic of the road under consideration in terms of accident correction with respect the base conditions; the Calibration Factors (C) that have the purpose of adjusting the model to take into consideration the actual condition of the analysed sites from the ones on which the HSM predictive model has been originally developed [26,27].

In accordance with the procedures in the HSM for each elementary segment of the highway under analysis, the following elements must be determined.

- *the safety performance functions* (SPF): functions to estimate the expected average crash frequencies in base conditions (that is, in the present infrastructure configuration) with regard to the annual average daily traffic on the highway segments in question;
- *the crash modification factors* (CMF): frequency correction factors calculated with SPF (in base conditions) to take the real geometric configuration into account (lane and hard shoulder widths, barrier presence, curve segment values, safety barrier location, etc.);
- *the expected average crash frequencies* per *unit for each route segment*, precisely:
  a) accident frequency per year and per kilometre with a single vehicle involved and damage only to property;
  b) accident frequency per year and per kilometre with a single vehicle involved and seriously or fatally injured people;
  c) accident frequency per year and per kilometre with multiple vehicles involved and damage only to property;
  d) accident frequency per year and per kilometre with multiple vehicles involved and seriously or fatally injured people;
- the *expected average* number of fire accidents that involve bridges.

It is useful to point out that according to the according with the HSM, an accident that produces “damage only to property” (commonly referred to as a Property Damage Only, PDO) are that designated by the severity code “O" in the KABCO scale, and denotes a traffic collision that results exclusively in structural or material damage to vehicles, roadside infrastructure, or other objects or structures, with no fatal or non-fatal personal injuries sustained by any involved party.

Accidents involving injuries do not exclude property damage, but the categories do not overlap in statistical reporting. Instead, they operate under a hierarchical mutual-exclusivity rule based on the highest level of severity.

2.2. Accidents prediction and model calibration

The predictive model for a motorway segment is based on the following analytical expressions suggested by the HSM:

$$N_{predicted} = N_{spf,x} \cdot (CMF_{1x} \cdot CMF_{2x} \cdot \ldots \cdot CMF_{mx}) \cdot C_x \quad (1)$$

where.

- $N_{spf,x}$: predicted crash frequency in the base conditions for the motorway segment x;
- $CMF_{1x} \cdot CMF_{2x} \cdot \ldots \cdot CMF_{mx}$: Crash Modification Factors evaluate for the motorway segment “x”;
- C_x: is the calibration factor;

Eq. (1) can be detailed as follows:

$$N_{p,fs,n,at,as} = N_{p,fs,n,mv,fi} + N_{p,fs,n,sv,fi} + N_{p,fs,n,mv,pdo} + N_{p,fs,n,sv,pdo} \quad (2)$$

$$N_{p,fs,n,mv,fi} = C_{fs,ac,mv,fi} \cdot N_{spf,fs,n,mv,fi} \cdot \left(CMF_{1,fs,ac,mv,fi} \cdot \ldots . CMF_{m,fs,ac,mv,fi}\right)$$

$$\cdot \left(CMF_{1,fs,ac,at,fi} \cdot \ldots . CMF_{m,fs,ac,at,fi}\right) \quad (3)$$

$$N_{p,fs,n,sv,fi} = C_{fs,ac,sv,fi} \cdot N_{spf,fs,n,sv,fi} \cdot \left(CMF_{1,fs,ac,sv,fi} \cdot \ldots . CMF_{m,fs,ac,sv,fi}\right)$$

$$x \left(CMF_{1,fs,ac,at,fi} \cdot \ldots . CMF_{m,fs,ac,at,fi}\right) \quad (4)$$

$$N_{p,fs,n,mv,pdo} = C_{fs,ac,mv,pdo} \; x \; N_{spf,fs,n,mv,pdo} \cdot \left(CMF_{1,fs,ac,mv,pdo} \cdot \ldots . CMF_{m,fs,ac,mv,pdo}\right)$$

$$\cdot \left(CMF_{1,fs,ac,at,pdo} \cdot \ldots . CMF_{m,fs,ac,at,pdo}\right) \quad (5)$$

$$N_{p,fs,n,sv,pdo} = C_{fs,ac,sv,pdo} \cdot N_{spf,fs,n,sv,pdo} \cdot \left(CMF_{1,fs,ac,sv,pdo} \cdot \ldots . CMF_{m,fs,ac,sv,pdo}\right)$$

$$\cdot \left(CMF_{1,fs,ac,at,pdo} \cdot \ldots . CMF_{m,fs,ac,at,pdo}\right) \quad (6)$$

where.

- $N_{p,fs,n,y,z}$: predicted average crash frequency of a freeway segment with n lanes, crash type y (y = sv: single vehicle, mv: multiple vehicle, at: all types), and severity z (z = fi: fatal and injury, pdo: property damage only, as: all severities) (crashes/yr);
- $N_{spf,fs,n,y,z}$: predicted average crash frequency of a freeway segment with base conditions, n lanes, crash type y (y = sv: single vehicle, mv: multiple vehicle, at: all types), and severity z (z = fi: fatal and injury, pdo: property damage only) (crashes/yr);
- $CMF_{m,fs,ac,y,z}$: crash modification factor for a freeway segment with any cross section ac, feature m, crash type y (y = sv: single vehicle, mv: multiple vehicle, at: all types), and severity z (z = fi: fatal and injury, pdo: property damage only);
- $C_{fs,ac,y,z}$: calibration factor for freeway segments with any cross section ac, crash type y (y = sv: single vehicle, mv: multiple vehicle, at: all types), and severity z (z = fi: fatal and injury, pdo: property damage only).

Equation (2) shows that the sum of four distinct rates gives the expected accident frequency: a) accidents with multiple vehicles involved and fatal and non-fatal casualties; b) accidents with a single vehicle involved and fatal and non-fatal casualties; c) accidents with multiple vehicles involved and damage only to property; d) accidents with a single vehicle involved and damage only to property. These frequency rates are to be calculated with Equation (3) ÷ (6).

The SPFs for multiple-vehicle crashes on freeway segments are expressed by the following equation:

$$N_{spf,fs,n,mv,z} = L^* \cdot \exp\left(a + b \cdot \ln[c \cdot AADT]\right) \quad (7)$$

$$L^* = L_{fs} - \left(0.5 \cdot \sum_{i=1}^{2} L_{en,seg,i}\right) - \left(0.5 \cdot \sum_{i=1}^{2} L_{ex,seg,i}\right) \quad (8)$$

where.

- $N_{spf,fs,n,mv,z}$ predicted average multiple-vehicle crash frequency of a freeway segment with base conditions, n lanes, and severity z (z = fi: fatal and injury, pdo: property damage only) (crashes/yr);
- L* effective length of freeway segment (mi);
- L_{fs} length of freeway segment (mi);
- $L_{en,\ seg,\ i}$ = length of ramp entrance i adjacent to subject freeway segment (mi);
- $L_{ex,\ seg,\ i}$ = length of ramp exit i adjacent to subject freeway segment (mi);
- a, b = regression coefficients;
- c = 0.001 is the AADT scale coefficient;
- AADT = Annual average daily volume of freeway segment (veh/day).

The SPFs for single-vehicle crashes on freeway segments are given following equation:

$$N_{spf,fs,n,sv,z} = L^{*} \cdot \exp\left(a + b \cdot \ln[c \cdot AADT]\right) \quad (9)$$

where:

$N_{spf,fs,n,sv,z}$ = predicted average single-vehicle crash frequency of a freeway segment with base conditions, n lanes, and severity z (z = fi: fatal and injury, pdo: property damage only) (crashes/yr).

The coefficient values are provided in the HSM, while the base conditions for the SPFs for multiple-vehicle and Single-Vehicle crashes on freeway segments are summarised in Table 1.

Once we obtained the expected average crash frequencies per kilometre under base conditions and calculated the crash modification factors for the actual geometric configuration of each motorway segment, we determined the expected average crash frequencies per kilometre per segment at varying AADT.

A CMF is a multiplicative factor or function used to estimate the change in crash frequency associated with a specific site condition. More specifically.

- CMF > 1, if site-specific conditions are worse than 'base' conditions;
- CMF $= 1$, if site-specific conditions are the same as 'base' conditions;
- CMF < 1, if site-specific conditions are better than 'base' conditions.

Table A. 1 shows the CMFs equations.

The product of SPF and CMF becomes uncalibrated predicted crash frequency. Therefore, HSM recommends deriving calibration factors using randomly selected 30 to 50 roadway sites that experienced a minimum of 100 crashes per year [30,31].

Although this process ensures that crash estimates are locally relevant, predictions for individual locations may still be influenced by the data aggregation process; consequently, alternative calibration approaches incorporating multiple calibration factors have been proposed [32]. According to the HSM method, crashes must be classified into the following types.

- the yearly crash frequency per kilometre with a single vehicle involved and damage only to property;
- the yearly crash frequency per kilometre with a single vehicle involved and people seriously or fatally injured;
- the yearly crash frequency per kilometre with multiple vehicles involved and damage only to property;
- the yearly crash frequency per kilometre with multiple vehicles involved and seriously or fatally injured people.

The calibration factors are calculated by dividing the total observed crashes by the total predicted crashes, as denoted in the following equations:

Table 1
Base conditions for the SPFs (adapted from the HSM manual).

Multiple-Vehicle Crashes	Single-Vehicle Crashes
- Length of horizontal curve 0.0 mi (i.e., not present) - Lane width 12 ft - Inside shoulder width (paved) 6 ft - Median width 60 ft - Length of median barrier 0.0 mi (i.e., not present) - Number of hours where volume exceeds 1000 veh/h/ln None - Distance to nearest upstream ramp entrances more than 0.5 mi from segment - Distance to nearest downstream ramp exits More than 0.5 mi from segment Length of Type B weaving section 0.0 mi (i.e., not present)	- Length of horizontal curve 0.0 mi (i.e., not present) - Lane width 12 ft - Inside shoulder width (paved) 6 ft - Median width 60 ft - Length of median barrier 0.0 mi (i.e., not present) - Number of hours where volume exceeds 1000 veh/h/ln None - Outside shoulder width (paved) 10 ft - Length of shoulder rumble strip 0.0 mi (i.e., not present) - Clear zone width 30 ft - Length of outside barrier 0.0 mi (i.e., not present)

$$C_{w,x,y,z} = \frac{\sum_{i=1}^{n_{sites}} \sum_{j=1}^{n_c} N_{o,w(i),x(i),y,z,j}}{\sum_{i=1}^{n_{sites}} \sum_{j=1}^{n_c} N_{p,w(i),x(i),y,z,j}} \quad (10)$$

where.

- $C_{w,\ x\ y,\ z}$ = calibration factor to adjust SPF for local conditions for site type *w*, cross-section or control type *x*, crash type *y*, and severity *z*;
- n_{sites} = number of sites;
- n_c = number of years in the crash period (yr);
- $N_{o,\ w(i),\ x(i),\ y,\ z,\ j}$ = observed crash frequency for site i with site type w(i) and year j (includes cross section or control type x(i) for crash type y and severity z) (crashes/yr);
- $N_{p,\ w(i),\ x(i),\ y,\ z,\ j}$ = predicted average crash frequency for site i with site type w(i) and year j (includes cross section or control type x (i) for crash type y and severity z) (crashes/yr).

The calibration of crash prediction models is essential to ensure their reliable transferability across different road networks. In particular, the direct application of the Highway Safety Manual (HSM) Safety Performance Functions (SPFs) to non-U.S. motorway networks, without appropriate calibration, may result in substantial systematic biases. Such biases may stem from differences in fleet composition, geometric design standards, traffic operating conditions, and crash reporting practices between U.S. and European road networks. The primary sources of prediction error include the underestimation of rear-end crashes, especially during traffic-flow breakdowns and stop-and-go conditions in peak periods; spatial misallocation of crash risk; and substantial differences in planimetric and vertical alignment, as well as geometric design standards, between U.S. and European motorways.

2.3. Fire risk analysis

The fire risk of a bridge is defined as a function of two components: the probability of occurrence of the fire event, and the associated consequences, representing the damage resulting from the event $R = P \times C$. The probability component is defined in terms of the fire-event frequency, estimated for each basic segment of the analysed motorway according to the HSM-based procedure. To determine the expected number of fire events occurring beneath an overpass over its design life, the expected fire-related crash frequency for each basic segment, expressed in accidents/(km·year), must be multiplied by the average width of the overpasses considered and by the assumed useful life (e.g. 50 years). The expected fire frequency must be further disaggregated according to fire severity, namely High Fire Intensity (HFI), Moderate Fire Intensity (MFI), and Low Fire Intensity (LFI), and according to the fire location on the carriageway, namely Lateral Position (LP), Central Position (CP), and Other Position (OP).

In this research, fire consequences are assessed for two representative bridge typologies of the motorway under study: a steel-concrete composite girder overpass and a steel arch overpass with an orthotropic deck. For each typology, representative fire

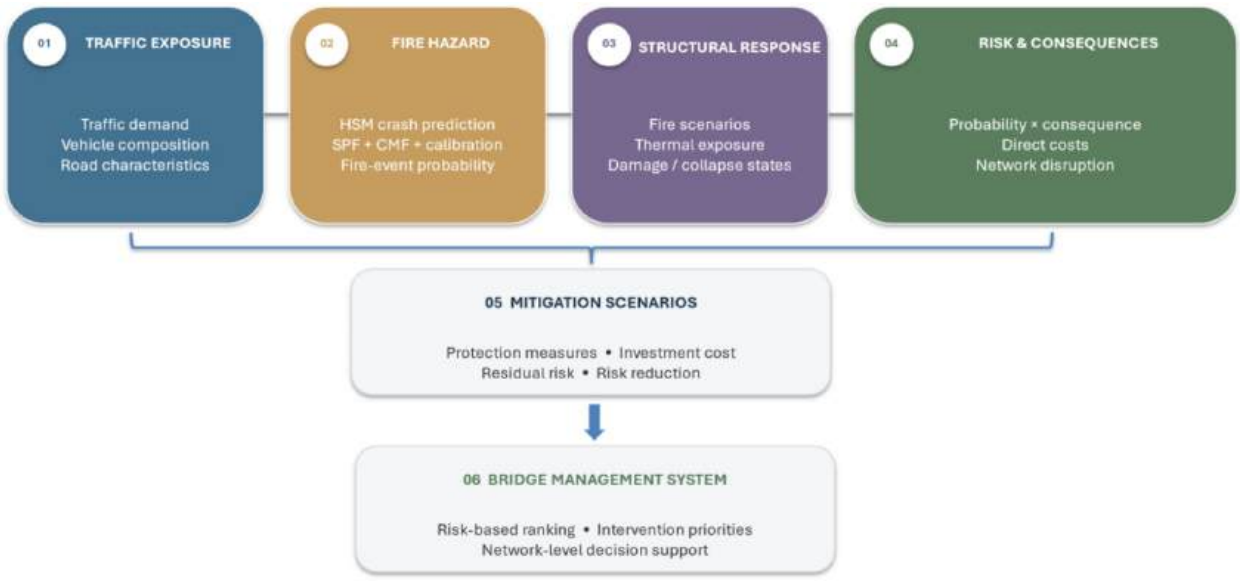


Fig. 1. Bridge fire risk methodology.

scenarios were defined considering different fire locations and both nominal and natural fire curves, including CFD-based simulations of Heavy Good Vehicles (HGV) fires. The resulting thermal actions were used in coupled thermo-mechanical analyses to evaluate structural deformation, failure modes, collapse time, and potential loss of functionality.

The consequences were then quantified through eight representative fire scenarios, accounting for direct and indirect costs, including intervention and traffic-disruption effects. The resulting costs were evaluated for each motorway basic segment as a function of fire intensity and location. Finally, the fire risk for each bridge and motorway segment was subsequently obtained by combining the estimated probability of fire occurrence with the corresponding economic consequences. The resulting risk profiles, differentiated by bridge typology and vehicle class, provide a basis for identifying critical locations and prioritising fire-risk mitigation measures, including active and passive fire-protection systems. Fig. 1 illustrates the bridge fire risk methodology.

3. Case study

The case study focuses on an important motorway belonging to the Helsinki–Valletta Corridor of the Trans-European Transport Network (TEN-T), as defined in Regulation (EU) No 1316/2013 [33]. This motorway is subject to "Directive 2008/96/CE of the European Parliament and Council on road infrastructure safety management", which requires an obligation to perform the Road Safety Impact Assessment (RSIA) for road infrastructure interventions and traffic management.

The analysed motorway has a total length of approximately 300 km, comprising 25 toll booths and an important interchange. The cross-section consists of two lanes in each direction, each 3.75 m wide, with right-hand hard shoulders 3.50 m wide and a 1.20 m-wide median. The horizontal alignment has 304 straight segments (minimum length $L_{min} = 1.55$ m, maximum length $L_{max} = 3331$ m) and 304 curves (minimum radius $R_{min} = 300$ m, maximum radius $L_{max} = 10{,}000$ m, minimum curve length $S_{min} = 29.83$ m, maximum curve length $S_{max} = 2{,}1088$ m).

3.1. The analysed motorway

Data collection on highway characteristics (vertical and horizontal alignments, cross section, volume data, traffic control features, etc.) and the segmentation process have been carried out according to the HSM Supplement instructions [34]. Interchanges, ramps and ramp terminals were excluded from the analysis. Data were collected for each motorway's travel direction, assuming the smallest segment length of 0.1 miles (160 m), and ignoring from the inspection some particular segments with uncommon features (i.e. segments with weaving sections, segments in which the number of lanes changes, etc.). According to the HSM method, the collected accident data were classified by crash severity (fatal and injury crashes or property-damage-only crashes) and by type (single- or multi-vehicle crashes). The analysis focused on fatal and injury crashes for both single- and multiple-vehicle accidents. Additionally, accidents below bridges with and without fire events were collected.

3.2. Traffic data and fire accident data

Statistical data from vehicle fires that occurred in 14 years (2010-2023) along the analysed motorway were collected and analysed in terms of location, damage intensity, time, vehicle type, presence of an overpass or a bridge, distance from a fire station and, where possible, the type of fire load, ignition causes and multimedia files of the fire event. A geographic information system (GIS) was created to store all the data. For example, Fig. 2 shows the vehicle fire accidents grouped by year and vehicle category extracted from the GIS.

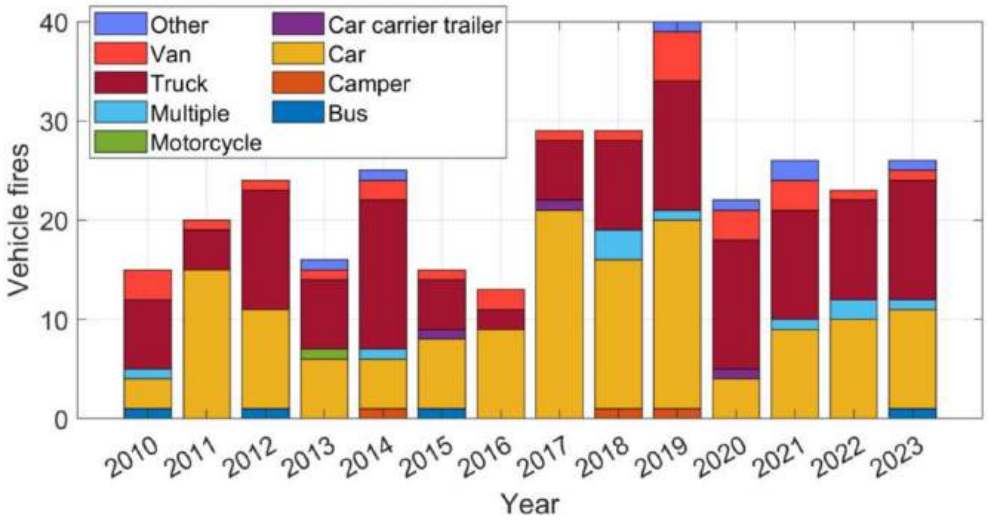


Fig. 2. Vehicle fire accidents on the analysed highway extracted from the GIS.

The vehicle fires observed between the 14 years mostly affected cars and heavy goods vehicles (HGVs).

To estimate the safety conditions of the motorway, the following analyses were carried out.

1. the analysed motorway was subdivided into 25 basic segments (Table 2), each with a constant AADT value;
2. the horizontal, vertical alignment and the cross-section of each segment were analysed according to the HSM methods (curvature, lane, hard shoulder and central reservation widths; safety barrier position with regard to hard shoulders, etc.);
3. traffic flow parameters were deducted, and the levels of services (LOS) were calculated with the HCM method;
4. HSM procedure was applied in order to estimate incidents with a particular focus on fire accidents near bridges;

For the purposes of this study, vehicles were classified into main two categories: light vehicles, including cars, motorcycles, vans, pickups, and multiple-vehicle accidents involving only light vehicles (e.g., car–car and car–motorcycle collisions); and heavy vehicles, including trucks, buses, campers, carrier trailers, tankers, and multiple-vehicle accidents involving at least one heavy vehicle (e.g., truck–car and truck–camper collisions). Accidents near bridges, considers both accidents involving property damage only and accidents resulting in the injury or death of road users.

Table 2 shows the AADT value, obtained as the mean of years 2010-2019 and 2022-2023, for each of the 25 basic segments of the analysed motorway, along with the relative percentages of light and heavy vehicles. The years 2020 and 2021 were excluded, as they were affected by restrictions that significantly influenced traffic patterns and, consequently, accident events. AADT ranges from 42848 veh/day to 66003 veh/day, and the percentage of heavy vehicles ranges from 44% to 56%. The number of observed crashes, accident rates, and the locations of observed crashes that result in fires are shown in Figs. 3 and 4.

Accident rates in Fig. 3c have been obtained as follows. First, the statistical accident data recorded on each motorway section that determined fires have been collected for the years 2010- 2023. The data was divided into accidents involving light and heavy vehicles. The accident frequency per section (expressed in accidents/(km·year)) for both light and heavy vehicles has been obtained.

An important factor to consider is the position of the fire on the motorway cross-section, as this affects the extent of the damage to the bridge. Given the fact that flexure often governs the bridge design, when a fire occurs near the midspan of a bridge, there are more significant effects on its structural integrity than those observed if the fire is located at the edges. The fires that occurred in the emergency lanes, in the lay-bys and in the entry lanes near ramps were aggregated into a single category called “lateral position”; those that occurred in the ordinary lanes (right and left lanes) are called “central position”, while those that occurred in the remaining areas were aggregated into a single category called “other”.

4. Application of the HSM to fire accidents

Fig. 5 shows the first result, which concerns the determination of SPFs (expected number of accidents per kilometre per year under basic conditions) as a function of AADT (Table A. 2). The values were then differentiated for light and heavy vehicles, in proportion to the percentages of light vehicles and heavy vehicles of each basic segment of the motorway, as summarised in Table A. 3 and Table A.

Table 2
AADT values of the motorway basic segments.

N°	Length (km)	AADT (veh/day)	Light vehicle percentage	Heavy vehicle percentage
1	16	42848	44%	56%
2	22	45839	45%	55%
3	10	50861	45%	55%
4	5	49055	45%	55%
5	24	52740	47%	53%
6	8	51265	46%	54%
7	16	60955	48%	52%
8	20	61837	49%	51%
9	10	61051	49%	51%
10	5	55195	50%	50%
11	6	53605	51%	49%
12	16	62119	54%	46%
13	9	63058	52%	48%
14	12	64764	51%	49%
15	28	65275	51%	49%
16	19	50726	56%	44%
17	3	63546	56%	44%
18	16	66003	51%	49%
19	13	64367	52%	48%
20	9	64291	51%	49%
21	12	64661	50%	50%
22	9	57618	51%	49%
23	17	58367	50%	50%
24	10	62876	52%	48%
25	1	64018	51%	49%

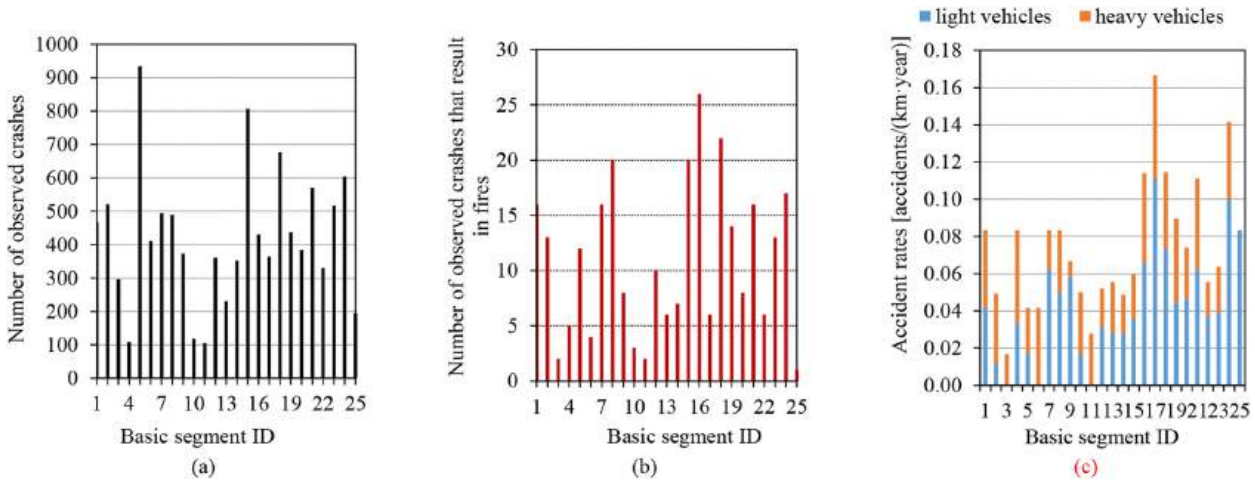


Fig. 3. a) Total number of observed accidents; b) number of observed crashes that result in fires; c) accident rates that result in fires (period 2010-2023).



Fig. 4. Location of the observed crashes that result in fires (period 2010-2023).

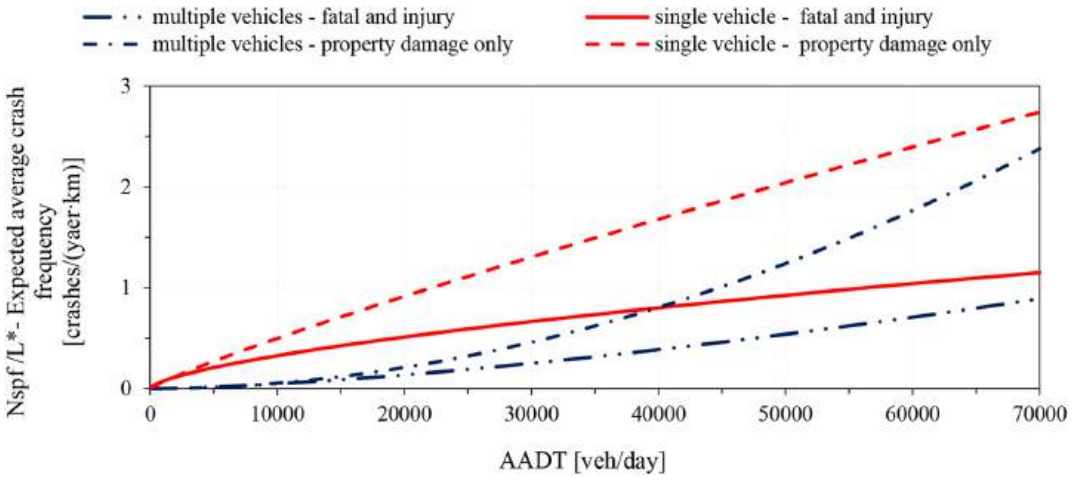


Fig. 5. Expected average crash frequency in basic condition.

4.

Based on the geometric characteristics of the analysed motorway, traffic levels (Table 2) and the equations in Table A. 1, the CMFs summarised in Table A. 5 have been obtained for each basic segment of the motorway. The model was calibrated using Equation (10) taking into account accidents that occurred over a twelve-year period (years 2010-2019 and 2022-2023). The years 2020 and 2021 were excluded, as they were affected by coronavirus pandemic-related restrictions that significantly influenced traffic patterns and, consequently, accident events. Then, the calibrated model was applied to predict the expected number of accidents resulting in fires with a 5-year projection, once the evolution of AADTs was established from the analysis of traffic time series for each motorway segment.

More comprehensively, the expected number of fire-related accidents was derived from historical accident data, separately for light and heavy vehicles, and expressed as annual frequencies per kilometre for each basic segment. For the 5-year projection, segment-specific linear regression models were used to estimate future light- and heavy-vehicle traffic; therefore, the heavy-vehicle proportion was not assumed constant but varied by segment according to the historical trends.

Considering the average motorway longitudinal slope and the most common length of heavy vehicles, according to the HCM manual [35], the projected heavy-vehicle traffic was converted into equivalent light-vehicle traffic using an equivalence coefficient of 2.5, and the resulting traffic volumes were used to calculate the SPFs and, subsequently, the predicted fire frequencies after applying CMFs and calibration factors. This approach implicitly assumes that the historical linear traffic trends remain representative over the five-year projection period. Results are given in Fig. 6.

In addition, a significant increase, on the order of 30%, in fire accidents associated with heavy vehicles is observed, particularly across the northern motorway segments, extending from Basic Segment 1 to Basic Segment 12.

The entire investigation process, demolition and reconstruction of a bridge damaged by fire can take months or years, during which traffic must be diverted to alternative routes, causing significant repercussions on mobility and users' costs. In the case of major motorways, the closure of a bridge could make it difficult to access essential services such as education, work, and health care, and reduce the flow of goods and services. Furthermore, diverting traffic to alternative routes can lead to increased traffic and longer travel times, thereby causing congestion, pollution, and accidents.

The temporary closure of a motorway overpass may cause significant inconvenience to the motorway and correlated costs, which must undergo partial or total closures to allow for work, namely:

It is, therefore, possible to define two types of cost [36].

- Direct costs: the costs incurred by the road operator, i.e. the costs of demolition and reconstruction of infrastructure-damaged facilities (bridges, pavement, safety barriers, and other structures) as well as the costs of related to the reduction of revenues from motorway tolls (cash inflows directly paid by users);
- Indirect costs: the costs incurred by road users, which can be quantified by the modified travel distance e and time required for each journey.

Indirect costs were calculated starting from the values of the macroscopic traffic variables associated with the motorway (in particular space mean speed and travel time) under the hypotheses of with and without roadworks by using the method of the Highway Capacity Manual [35].

In light of these considerations, the following two standard scenarios were analysed.

- *Scenario 0*: corresponds to the configuration of the motorway in ordinary traffic conditions of use (two lanes in each direction of travel);

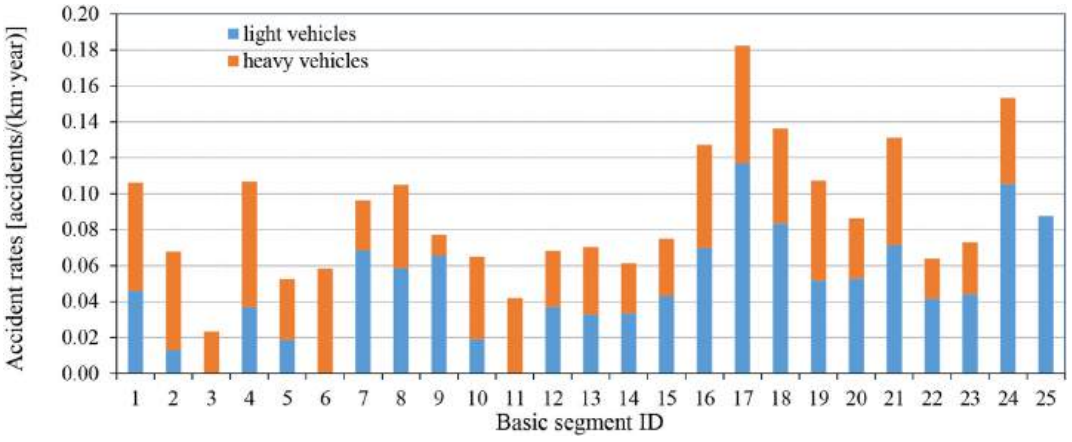


Fig. 6. Predicted accident rates that result in fires with a 5-year future traffic projection.

- *Scenario 1:* corresponds to the post-fire configuration of an overpass bridge in which the partial closure of the carriageway is necessary to allow for the various work activities within the motorway. In this scenario, only one lane in each direction of travel is considered.

The hourly traffic volumes for each carriageway and each motorway segment were recorded by the road operator.

Table 3 and Table 4 present the performance analysis, in terms of Level of Service (LOS) results for the motorway during the afternoon peak traffic hour (17:00-18:00) on a weekday. The level of service is a measure of traffic flow quality. For a motorway section, the LOS is estimated from the following main input parameters: number of lanes per direction (N); Peak Hourly Volume (VHP in veh/h); Heavy Vehicle Adjustment Factor (f_{hw}), space mean speed ($\overline{V}$ in km/h) and vehicle density (K in veh/km). The traffic flow conditions which characterise each level of service can be described as follows:

- LOS A, free flow with no mutual vehicle conditioning: very low vehicle density, very high driving comfort;
- LOS B, stable flow: low density which imposes relatively rare restrictions on freedom of manoeuvre; however, drivers always enjoy considerable freedom of choice in speed as well as in driving lanes; phase B is still in reasonably free flow conditions with high driving comfort;
- LOS C, still a stable flow: increase in density values; greater conditioning between vehicles. Fairly frequent lane-changing and/or overtaking in order to maintain the desired speed; the average speed attained is, however, still satisfactory; still acceptable driving comfort;
- LOS D, approaching unstable flow: high density and reduced freedom of manoeuvre; still mostly stable operational conditions; acceptable average speeds even if strongly influenced by changes in traffic flow conditions; poor driving comfort;
- LOS E, unstable flow: nearly the same traffic flow as the capacity value; very high density; virtually zero driving freedom; any perturbation in the traffic flow brings about rapid speed drops to a complete standstill; extremely poor driving comfort;
- LOS F, forced or breakdown flow: density at its highest values; vehicles move up in the queue under stop-and-go conditions; by far the poorest standards in driving conditions.

For a motorway under uninterrupted traffic conditions, LOS are related only to the vehicle density (K = 0-7 veh/km, LOS A; K = >7-11 veh/km, LOS B; K = >11-16 veh/km, LOS C; K = >16-22 veh/km, LOS D; K > 22-28 veh/km, LOS E; K > 28 veh/km, LOS F).

As can be seen, in Scenario 1 (closure of a lane on each carriageway to carry out maintenance/reconstruction activities on an accidented overpass), the space mean speed decreases relative to Scenario 0, and the LOS significantly worsens. It is observed that in Scenario 1, many segments reach congestion (i.e. LOS F).

Table 3
Traffic flow variables and LOS. Scenario 0, weekday (time interval 17:00-18:00).

Basic Segment n°	N [−]	Southward						Northward					
		VHP [veh/h]	f_{HV} [−]	Q [veh/h/lane]	$\overline{V}$ [km/h]	K [veh/km/lane]	LOS	VHP [veh/h]	f_{HV} [−]	Q [veh/h/lane]	$\overline{V}$ [km/h]	K [veh/km/lane]	LOS
1	2	1039	0.75	771	110	7.01	B	1130	0.31	2055	101	20.40	D
2	2	1347	0.89	838	110	7.62	B	1250	0.57	1216	110	11.05	C
3	2	1316	0.88	829	110	7.54	B	1366	0.39	1948	104	18.66	D
4	2	1272	0.71	990	110	9.00	B	1320	0.60	1226	110	11.15	C
5	2	1488	0.89	931	110	8.46	B	1469	0.64	1284	110	11.67	C
6	2	1211	0.83	809	110	7.35	B	1333	0.61	1212	110	11.02	C
7	2	1882	0.90	1168	110	10.62	B	1477	0.85	966	110	8.78	B
8	2	1917	0.89	1192	110	10.84	B	1651	0.85	1080	110	9.82	B
9	2	1820	0.89	1139	110	10.35	B	1650	0.85	1079	110	9.81	B
10	2	1654	0.89	1035	110	9.41	B	1499	0.85	981	110	8.92	B
11	2	1532	0.90	949	110	8.63	B	1688	0.86	1085	110	9.86	B
12	2	1999	0.86	1286	110	11.69	C	2050	0.82	1394	110	12.67	C
13	2	1805	0.74	1349	110	12.26	C	1989	0.68	1624	110	14.81	C
14	2	1604	0.90	994	110	9.04	B	2059	0.87	1320	110	12.00	C
15	2	2390	0.73	1814	108	16.87	D	2078	0.69	1673	109	15.31	C
16	2	1716	0.68	1403	110	12.75	C	1676	0.67	1394	110	12.67	C
17	2	2145	0.86	1379	110	12.54	C	2095	0.86	1357	110	12.34	C
18	2	1929	0.90	1195	110	10.86	B	2376	0.72	1824	107	16.99	D
19	2	1811	0.82	1224	110	11.13	C	2266	0.82	1539	110	14.00	C
20	2	1683	0.90	1044	110	9.49	B	1365	0.96	793	110	7.21	B
21	2	895	0.96	519	110	4.72	A	2282	0.90	1415	110	12.86	C
22	2	813	0.84	536	110	4.87	A	2048	0.94	1212	110	11.02	C
23	2	1485	0.90	922	110	8.38	B	1931	0.90	1192	110	10.84	B
24	2	1398	0.84	924	110	8.40	B	1932	0.81	1327	110	12.06	C
25	2	1585	0.90	983	110	8.94	B	2035	0.68	1652	109	15.09	C

Table 4
Traffic flow variables and LOS. Scenario 1, weekday (time interval 17:00-18:00).

Basic Segment n°	N [−]	Southward						Northward					
		VHP [veh/h]	f_{HV} [−]	Q [veh/h/lane]	$\overline{V}$ [km/h]	K [veh/km/lane]	LOS	VHP [veh/h]	f_{HV} [−]	Q [veh/h/lane]	$\overline{V}$ [km/h]	K [veh/km/lane]	LOS
1	1	1039	0.75	1542	110	14.03	C	1130	0.31	4111	10	411.10	F
2	1	1347	0.89	1675	109	15.33	C	1250	0.57	2432	10	243.20	F
3	1	1316	0.88	1658	109	15.15	C	1366	0.39	3896	10	389.60	F
4	1	1272	0.71	1980	103	19.15	D	1320	0.60	2452	10	245.20	F
5	1	1488	0.89	1861	107	17.46	D	1469	0.64	2567	10	256.70	F
6	1	1211	0.83	1618	110	14.75	C	1333	0.61	2424	10	242.40	F
7	1	1882	0.90	2335	85	27.46	E	1477	0.85	1932	105	18.42	D
8	1	1917	0.89	2384	10	238.40	F	1651	0.85	2161	96	22.54	E
9	1	1820	0.89	2278	89	25.59	E	1650	0.85	2159	96	22.49	E
10	1	1654	0.89	2070	100	20.68	D	1499	0.85	1962	104	18.87	D
11	1	1532	0.90	1898	106	17.95	D	1688	0.86	2170	95	22.75	E
12	1	1999	0.86	2571	10	257.10	F	2050	0.82	2788	10	278.80	F
13	1	1805	0.74	2697	10	269.70	F	1989	0.68	3248	10	324.80	F
14	1	1604	0.90	1989	103	19.29	D	2059	0.87	2639	10	263.90	F
15	1	2390	0.73	3627	10	362.70	F	2078	0.69	3346	10	334.60	F
16	1	1716	0.68	2807	10	280.70	F	1676	0.67	2789	10	278.90	F
17	1	2145	0.86	2758	10	275.80	F	2095	0.86	2714	10	271.40	F
18	1	1929	0.90	2390	10	239.00	F	2376	0.72	3648	10	364.80	F
19	1	1811	0.82	2447	10	244.70	F	2266	0.82	3078	10	307.80	F
20	1	1683	0.90	2087	99	21.00	D	1365	0.96	1585	110	14.43	C
21	1	895	0.96	1037	110	9.43	B	2282	0.90	2831	10	283.10	F
22	1	813	0.84	1073	110	9.75	B	2048	0.94	2424	10	242.40	F
23	1	1485	0.90	1843	107	17.23	D	1931	0.90	2383	10	238.30	F
24	1	1398	0.84	1847	107	17.28	D	1932	0.81	2654	10	265.40	F
25	1	1585	0.90	1965	104	18.91	D	2035	0.68	3303	10	330.30	F

4.1. Indirect cost estimation

The indirect costs associated with the maintenance/reconstruction activities of a damaged overpass can be quantified based on the space travelled by each user and the time spent for each trip, which may increase due to roadworks. The estimated costs are indicative; their purpose is to illustrate the procedure rather than represent exact values.

The estimation of indirect costs is based on the following simplifying assumptions.

- the same average length of the roadworks-affected area is assumed for all overpasses;
- the speeds of both light and heavy vehicles are assumed to be equal to the average space mean speed of the traffic flow, as calculated using the macroscopic traffic-flow models described in the Highway Capacity Manual (HCM);
- average travel time is assumed to be independent of trip purpose (e.g., business, leisure, tourism);
- traffic demand is assumed to remain constant between Scenario 0 and Scenario 1. This implies that, during the roadworks, users are assumed to continue using the motorway under consideration rather than diverting to alternative roads or routes, where available;
- the transition from Scenario 0 to Scenario 1 does not involve any change in the distance travelled by each user but does involve an increase in travel times due to roadworks;
- the hourly traffic flows for each basic segment were derived from typical traffic conditions on the motorway (two weekdays and one public holiday); therefore, the estimated indirect costs may vary on days characterised by traffic flows different from those assumed as the basis for the analysis.

Assuming a mean length of the impact of the area roadworks is 1 km, the increase in travel time that all users of a given time interval experience following the closure of a lane of the carriageway can be calculated with the following expression:

$$\Delta t_{i,j} = \left(t_{1,i,j} - t_{0,i,j}\right) \cdot VH_{i,j} \tag{11}$$

where.

- $t_{1,i,j} = \frac{1\ km}{\overline{V}_{1,i}}$ is the travel time, expressed in hours, taken to travel 1 km of the basic segment j, in Scenario 1 and in time slot i;
- $t_{0,i} = \frac{1\ km}{\overline{V}_{0,i}}$ is the time, expressed in hours, taken to travel 1 km of the basic segment j in Scenario 0 and in time slot i;
- $VH_{i,j}$ is the hourly flow rate of the basic segment j in time slot *i*.

Travel time increases due to both non-work and work activities, representing one of the most significant costs associated with

demolishing the damaged overpass and constructing a new one.

Under the assumption of constant traffic demand (i.e., no traffic diversion from Scenario 0 to Scenario 1) and using an average value of travel time of €18/h [37] together with hourly traffic flow data for two typical weekdays and one holiday, the indirect travel time costs were estimated as reported in Table 5, based on the application of macroscopic traffic flow models from the Highway Capacity Manual (HCM, 2022).

The construction schedule assumes that the most disruptive works are carried out during off-peak hours and nighttime intervals to minimize traffic disruption.

4.2. Direct costs estimation

The direct costs examined in the study include the costs of demolition and reconstruction of the damaged bridge, the loss of toll revenues, the costs of replacing the flexible road pavement (surface, binder and base courses whose thicknesses are 6 cm, 7 cm, and 32 cm, respectively) and the metallic safety barriers (H3 type) damaged following an accident that results in fire. As stated previously, the estimated costs are approximate and intended only to illustrate the procedure, not to represent exact values; the estimates are based on reports and publicly available price lists (e.g., the Italian highways agency (ANAS) price list). The following hypotheses are considered, taking into account the damage of previous fire accidents along the analysed motorway.

- damaged lengths of pavements and barriers: 30 m;
- unit costs of surface, binder and base courses: 229.67 €/m^3, 217.09 €/m^3, 192.36 €/m^3 respectively;
- unit cost of the lateral metallic safety barrier (H3 type): 195.22 €/m;
- unit cost of the central metallic safety barrier (H3 type): 406.23 €/m;
- different values of revenue tolls from light and heavy vehicles. It is assumed that the closure of the road to traffic is related to the nighttime interval (22:00 – 06:00).

Table 6 summarises the costs due to the loss of toll revenues.

5. Application of the fire risk analysis to the selected case study

5.1. Probability estimation

The probability is defined by the fire frequency, calculated using the HSM procedures for the basic segments. To obtain the number of fires expected under an overpass during its design life, it is necessary to multiply the expected crash fire frequencies of each basic segment (expressed in accidents/(km•year) by the average width of the analysed overpasses (15.0 m, plus 2.5 m per side beyond the edges of the deck) and by its design life (assumed 50 years). The expected frequency of fires was also divided according to the severity

Table 5
Indirect costs of the travel time (daytime time slots).

Basic Segment n°	Travel time costs [€] - Southward			Travel time costs [€] - Northward		
	weekday 1	weekday 2	holiday	weekday 1	weekday 2	holiday
1	1.15	0.00	0.00	27,575.55	17,558.91	24,493.94
2	9.35	0.00	17.87	9693.88	33.98	7007.47
3	9.30	0.10	10.95	20,994.98	21,402.11	24,826.48
4	189.77	73.26	140.78	6328.43	7.24	15,824.95
5	44.04	5.52	19.92	14,103.62	346.05	16,691.63
6	0.85	0.34	0.85	14,812.43	3295.25	14,812.43
7	403.23	135.93	77.41	9221.74	160.59	9788.79
8	4501.66	139.44	154.04	13,802.09	244.55	17,736.75
9	359.21	108.41	135.96	13,777.93	194.66	9574.08
10	124.07	28.15	43.56	8681.43	61.09	4669.01
11	68.03	3.73	60.57	4431.49	14.86	4501.99
12	16,715.88	330.98	8508.71	38,443.74	4199.43	14,123.61
13	35,094.43	27,415.47	12,433.50	43,929.73	28,527.50	21,346.32
14	346.26	116.53	4558.35	26,032.81	162.87	9861.81
15	28,606.63	28,411.62	12,591.88	44,017.64	27,970.60	18,255.23
16	3781.76	57.19	162.26	13,467.91	60.76	11,205.65
17	4721.19	80.89	3862.45	13,098.97	73.73	14,083.54
18	4526.94	4268.14	17.69	50,249.72	37,289.76	12,591.05
19	4167.60	142.47	138.18	30,063.49	257.01	12,624.57
20	256.25	148.00	6.99	0.67	0.00	0.00
21	0.00	0.00	0.00	23,059.93	216.43	4692.34
22	0.00	0.00	0.09	13,550.83	49.93	0.00
23	130.15	81.77	0.00	12,720.69	52.66	84.77
24	66.54	106.69	0.04	12,674.04	3891.29	151.79
25	305.15	100.58	4480.35	46,308.71	30,785.20	17,608.39

Table 6
Costs due to the loss of toll revenues during the nighttime interval (22:00 – 06:00).

Basic Segment n°	weekday 1	weekday 2	holyday
	Costs [€]	Costs [€]	Costs [€]
1	7671.57	7346.04	7286.18
2	10,637.20	10,952.00	10,609.50
3	6453.12	6645.20	6033.67
4	3863.70	4007.40	3813.90
5	13,291.00	13,653.00	12,898.60
6	4367.50	4253.70	4367.50
7	10,171.00	10,577.00	10,087.00
8	11,957.00	11,778.40	11,472.40
9	6408.00	6227.40	6204.30
10	4511.56	4388.90	3983.48
11	4924.91	4643.11	4924.82
12	11,135.70	10,245.20	10,559.90
13	5483.50	5168.10	5095.00
14	7720.50	6689.30	6866.30
15	16,961.10	15,707.50	14,972.30
16	4124.90	3864.30	4870.20
17	6970.13	6526.13	12,247.88
18	12,033.30	11,159.10	9845.40
19	6502.90	4865.10	6766.70
20	3113.40	2788.40	2682.20
21	3474.40	3067.00	2628.70
22	4198.80	3987.60	3236.70
23	8472.40	8124.80	6711.20
24	3365.60	2913.00	3463.20
25	4759.37	4107.95	4278.71

of the fire (High fire intensity (HFI), Moderate fire intensity (MFI), Low fire intensity (LFI), and its position on the carriageway (i.e. Lateral position (LP), Central position (CP), Other (OP)) by using the same proportion recorded in the past along the analysed motorway. Fig. 7 illustrates the results.

5.2. Consequences estimation

The accident consequences were determined by analysing two different types of overpasses: a girder overpass with a composite steel-concrete structure (Fig. 8a) and a steel arch overpass with an orthotropic steel deck (Fig. 8b). These typologies reflect the standardised bridge solutions currently adopted within the investigated motorway network. The steel-concrete composite girder overpass has a span length of 45 m and is used for the majority of crossings, whereas the steel arch overpass has a span length of 65 m

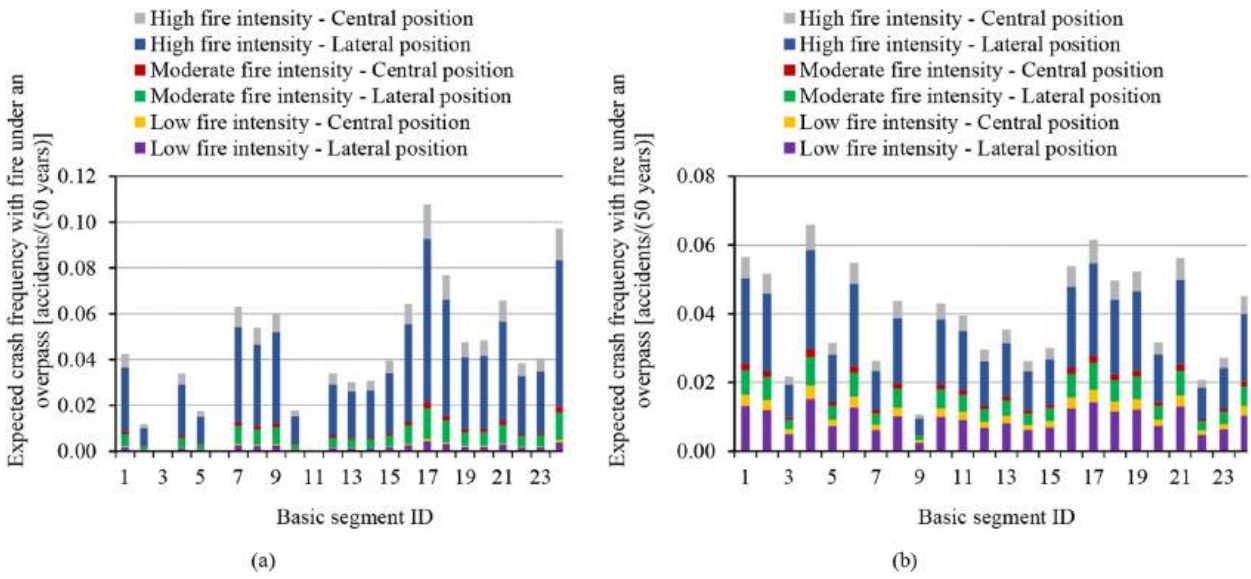


Fig. 7. Expected frequency of accidents under an overpass. a) accidents of light vehicles; b) accidents of heavy vehicles.



Fig. 8. a) Example of a girder overpass with a composite steel-concrete overpass. b) Example of a steel arch overpass.

and is mainly adopted in the vicinity of motorway entry and exit stations, where the presence of acceleration and deceleration lanes requires longer spans. The bridges belonging to the same typology exhibit similar geometric and structural characteristics throughout the network. Therefore, the use of representative models is considered appropriate for the network-level assessment.

Previous studies have demonstrated that girder bridges are more vulnerable to fires occurring beneath the bridge than arch overpasses [19,20]. In those studies, both prescriptive and performance-based fire design approaches were investigated through the adoption of nominal [38] and natural fire curves. In the present study, only the performance-based approach was adopted. Hence,the natural fire scenarios were derived from Computational Fluid Dynamics (CFD) simulations of vehicle fires of both light-vehicle and heavy-vehicle fires [39–41], as illustrated in Fig. 8. The corresponding heat release rate (HRR) curves were used as input for the CFD simulations. During the CFD analyses, adiabatic surface temperature (AST) devices were positioned beneath the overpasses to record the evolution of the gas temperature at different locations. The resulting temperature-time histories were subsequently used as thermal input for the thermal-structural analyses performed with SAFIR. The structural response obtained from these analyses, in terms of collapse, residual deformation, and loss of functionality, was then used to quantify the consequences associated with each fire scenario by means of nonlinear thermomechanical analyses. Fig. 9a presents the reference heat release rate (HRR) curves for a Class 3 car fire, with a peak HRR of 8.3 MW [39], and the HRR curve for a light commercial vehicle fire [40]. For commercial vehicles, the CTICM guidelines recommend a peak heat release rate of 18 MW. This value is intended as a conservative design value for fire safety assessments and does not correspond to a directly measured experimental value [40]. Fig. 9b illustrates the experimental heat release rate (HRR) curve of a heavy goods vehicle (HGV) loaded with wood and plastic pallets, with a peak HRR of 200 MW [41].

For brevity, one simulation is selected as an example of a CFD modelled scenario involving a HGV loaded with wood and plastic at the mid-span of the domain. Fig. 10a and b illustrate the development of fire and smoke after 22 min from the beginning of one fire scenario as an example of the fire development stages. Structural collapse of the girder bridge occurred after 23 min due to failure of the mid-span girders, whereas no structural failure was observed on the arch bridge, because the fire did not affect the arch structural capacity. Considering the natural fire curve, the residual deflections for the arch bridge are close to the L/250 limit identified by Ref. [42], whereas those for the nominal fire curves are significantly higher. These values do not allow to guarantee the full functionality of the structure. High deflections could prevent the bridge's opening at full traffic load, forcing the road operator to limit traffic loads, for example, allowing the transit of light vehicles only. In the case of an overpass, this problem also extends to the road below the structure (i.e. the motorway) since a high deflection could limit the passage of heavy vehicles. Consequently, in these cases, the demolition and reconstruction of the bridge could be necessary. The structural consequences associated with each fire scenario

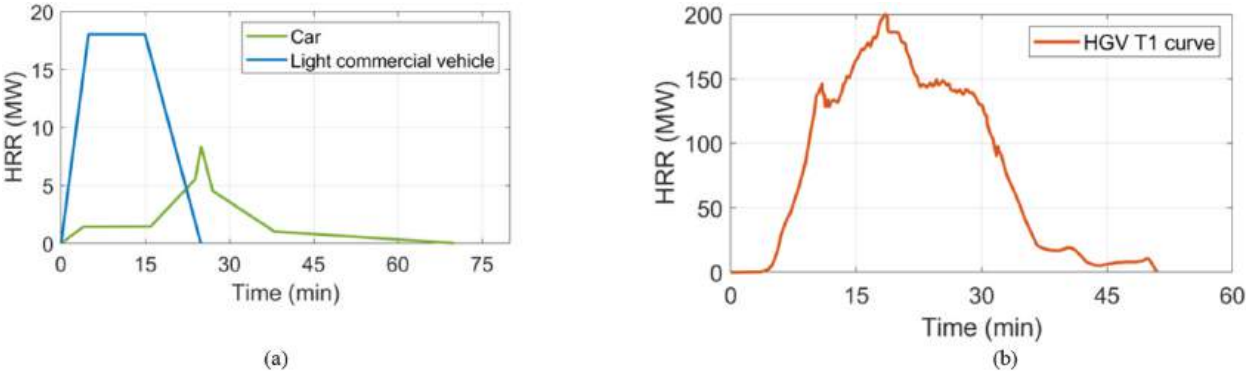


Fig. 9. Heat release rate of the natural curves: (a) example light vehicles (car and light commercial vehicle/utility vehicle) [39,40]. (b) Heavy goods vehicle (HGV) loaded with wood and plastic pallets [41].

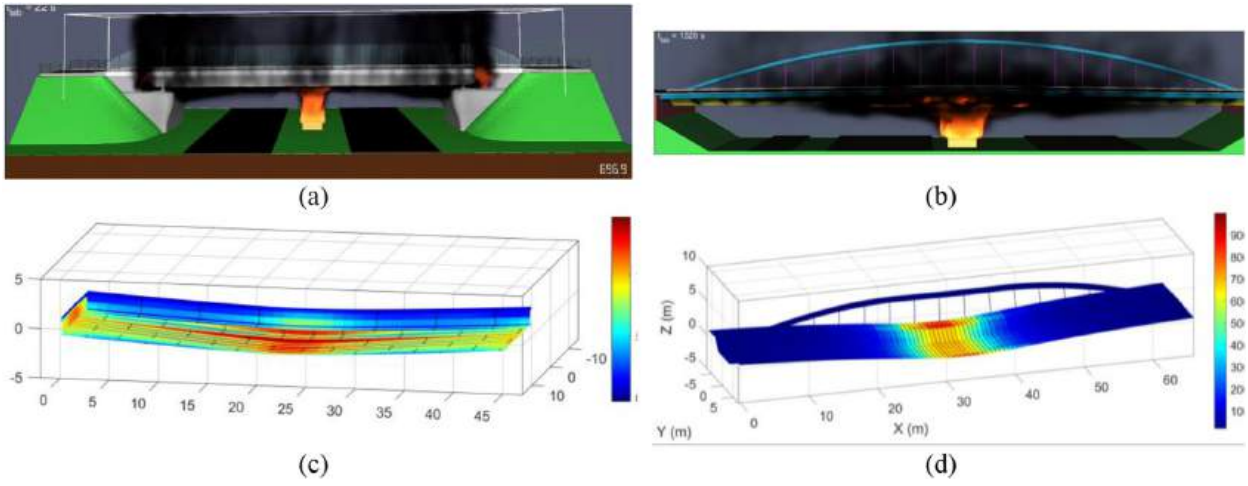


Fig. 10. View of the bridge after 22 min after the fire started: (a) FDS results general view of the girder overpass; (b) FDS results general view of the arch overpass; (c-d) Deformed shape and surface temperature of the overpasses.



Fig. 11. Examples of past fire accidents on motorways considered for illustrative purposes, showing different vehicle types, fire positions, and fire intensities (various sources, including fire and emergency services [43–47]).

were classified into damage states based on the results of the thermomechanical analyses and the extent of the bridge affected by the fire. The classification was performed according to the fire performance levels and associated limit states proposed by De Silva et al. [42], which consider both structural resistance and displacement criteria. The resulting damage states were then used to define the required post-fire interventions, ranging from inspection and repair activities to bridge demolition and reconstruction, and subsequently to estimate the corresponding direct and indirect costs.

The research considered eight different fire accident cases correlated with different types of direct, indirect, and total costs. It was assumed that an accident with fire occurred on weekday 1 since it was the busiest and therefore represented the most burdensome condition. The duration of the Fire Brigade intervention was determined based on statistical analyses of historical accident data collected across multiple motorways. This duration was used to define the period of the immediate partial or complete motorway closure following the accident and, consequently, to estimate the associated short-term direct and indirect costs. It was assumed that the construction activities are carried out on weekday 2 (less busy weekday). For illustrative purposes regarding the type of vehicles, position and intensity of fire considered in the eight scenarios, some examples of accidents that occurred in the past along motorways are shown in Fig. 11.

The eight scenario summaries for beam and arch bridges are reported in Table 7, which synthesize the range of fire-induced damage conditions analysed in this study. The scenarios are defined by combining traffic characteristics (light versus heavy vehicles), damage severity levels, and the position of the fire event, all of which significantly influence the extent of structural damage and the required interventions. The fire positions considered in this study, were selected based on observations of real vehicle-fire accident scenarios. In severe accidents, vehicles may come to rest close to the guard rails or median barrier, which act as containment systems, whereas in less severe accidents the vehicle may remain in the emergency lane after ignition. Accordingly, two representative fire positions beneath the overpass were considered: a central position and a lateral position. These configurations were selected to represent the most relevant scenarios identified from observed fire events and discussions with the motorway operator. The analysis therefore does not aim to reproduce the full spatial variability of possible fire locations, but rather to investigate representative scenarios associated with potentially significant structural consequences. The uncertainty associated with fire position and fire intensity is not explicitly considered in the present scenario-based framework; Preliminary results investigating these uncertainties through fire fragility functions have been presented in a related study in Ref. [48].

For each scenario, both estimated direct and indirect cost components are identified (Table 8 and Table 9). Direct costs include structural repairs, demolition and reconstruction activities, load testing, and replacement of bridge elements (Table 10), while indirect costs primarily reflect the impact on traffic flow, such as partial or full lane closures, duration of disruptions, and consequent loss of service. It should be noted that the assumptions adopted in this cost analysis are intended for estimation purposes and do not necessarily represent the actual procedures or operational practices implemented by the motorway operator.

Based on these assumptions, the overall costs for each basic segment were calculated, depending on the vehicle fire intensity and its position on the roadway. These costs are expressed in Figs. 12 and 13 as percentages of the estimated construction cost of the two analysed overpass type. Fig. 12a and b reveal a significant cost difference between the various basic segment, whereas the differences appear less pronounced in Fig. 13a and b, because the substantially higher direct costs associated with heavy-vehicle fire scenarios dominate the total cost, thereby reducing the relative influence of segment-specific factors. However, analysing the values, it is clear that between the most expensive highway segment, Segment 15 and the least expensive segment, Segment 20 (cf. Table 2) there is a difference of over €650,000 for the girder bridge and €790,000 for the arch bridge.

5.3. Risk estimation

At this point, since the probability of occurrence of a fire involving a bridge and the consequences in terms of costs are known, it is possible to compute the risk according to Eq. (12). Fig. 14 illustrates the risk associated with each segment, both for the girder bridge and the arch bridge, highlighting the risk related to light and heavy vehicles. The graphs clearly show that the risk component associated with light vehicles is negligible compared to that of heavy vehicles, due to the significantly lower consequences.

The result, in terms of risk, for the two different types of bridges is also reported in Fig. 15. This representation concerns the risk associated with a single overpass. However, the analysed motorway includes 150 overpasses, and most of the 25 basic segments of the motorway include multiple overpasses, resulting in a greater probability for the entire segment. For the sake of simplicity, all bridges are considered steel-concrete girder structures, except those located near the motorway entrances and exits, which were considered arch bridges. Based on these considerations, the total risk was calculated by multiplying the values summarised in Fig. 15 by the number of overpasses present in each basic segment. The results are summarised in Table 11 and Fig. 16a. Nevertheless, bridges belonging to the same typological category may exhibit different levels of fire vulnerability depending on their specific structural characteristics. Consequently, the estimated risk values should be interpreted as representative of the investigated motorway network rather than universally applicable to all bridges of the same typology. For networks characterised by a greater variety of bridge configurations, the proposed methodology should be calibrated using additional representative overpass-specific structural analyses.

These results can constitute a management tool to identify the cases in which it would be more appropriate to provide bridges with an adequate fire risk mitigation strategy, such as the application of the fire protection. Active or passive protection systems can be used to reduce the consequences of a fire on a bridge. Active protection is based on devices that intervene automatically in the event of a fire, such as water sprayers (sprinklers) or foam systems. For the case study under analysis, it was assumed the fire protection through the application of intumescent paint on bridges would be adopted as a fire risk mitigation strategy. Taking into account the unit cost of intumescent paint (€24,300.00/m^3), the surface area to be treated for each bridge type, and two applications over the useful life of the structure, the total protection cost amounts to €283,887.52 for the girder bridge and €147,598.49 for the arch bridge. The

Table 7
General description of the eight fire accident scenarios.

Scenario	Vehicle Type	Fire Intensity	Position	General case description
1	Light vehicles	Low/ Moderate	Lateral & Central	Flames are limited in extent. No damage to the bridge or road superstructure is expected.
2	Light vehicles	High	Lateral	More intense flames. Damage to later noise and safety barriers; no structural bridge damage.
3	Light vehicles	High	Central	No bridge damage expected, but damage to the central safety barrier was assumed.
4	Heavy vehicles	Low	Lateral & Central	Limited fire load. No damage to the bridge or road superstructure expected.
5	Heavy vehicles	Moderate	Lateral	Significant fire load; partial damage to the bridge is possible. Noise barriers, lateral safety barriers, and partial pavement replacement on one lane are expected.
6	Heavy vehicles	Moderate	Central	Similar to Scenario 5 but with more significant partial bridge damage due to the central position. Central safety barrier and partial pavement replacement on one lane expected.
7	Heavy vehicles	High	Lateral	Fire load sufficient to cause collapse of a girder bridge; partial damage to the arch bridge. Noise barriers, lateral safety barriers, and partial pavement replacement expected.
8	Heavy vehicles	High	Central	Collapse of girder bridge; severe damage to arch bridge. Central median barrier damage and full pavement replacement on the entire carriageway expected.

Table 8
Impacts of the eight light/heavy vehicle fire scenarios analysed regarding the girder bridge.

Scenario	Estimated Direct Costs	Estimated Indirect Costs
1	None	None, one lane (emergency or travel lane) closed for fire brigade; remaining two lanes kept open.
2	• Noise barriers • Lateral safety barriers	• Fire brigade (17:00–18:00, Weekday 1): emergency + travel lane closed for 1 h • Noise barrier replacement: only emergency lane closed; other 2 lanes open • Lateral barrier replacement (20:00–23:00, Weekday 2): emergency + travel lane closed for 3 h
3	• Central median barrier • Lost toll revenue: full carriageway closure for 1 h (17:00–18:00, Weekday 1)	• Median barrier replacement (22:00–06:00, Weekday 2): travel + overtaking lanes closed in both directions for 1 night; traffic on emergency lane
4	None	None, one lane (emergency or travel lane) closed for fire brigade; remaining two lanes kept open.
5	• Structural inspection & tests • Bridge load test • Lost toll revenue (load test, 22:00–06:00, Weekday 2): both carriageways closed for 1 night • Partial bridge repair (15% of construction cost) • Noise barriers • Lateral safety barriers • Pavement replacement (1 lane)	• Fire brigade (17:00–18:00, Weekday 1): emergency + travel lane closed for 1 h • Inspection/tests (08:00–20:00, Weekday 2): 2 lanes closed in busiest carriageway for 2 days • Partial bridge repair (08:00–20:00, Weekday 2): 2 lanes closed for 2 days • Noise barrier replacement: only emergency lane closed • Lateral barrier replacement (20:00–23:00, Weekday 2): emergency + travel lane for 3 h • Pavement replacement (20:00–23:00, Weekday 2): emergency + travel lane for 3 h
6	• Lost toll revenue: fire brigade (17:00–18:00, Weekday 1): full carriageway closed for 1 h • Structural inspection & tests • Bridge load test • Lost toll revenue (load test, 22:00–06:00, Weekday 2): both carriageways closed for 1 night • Partial bridge repair (20% of construction cost) • Central median barrier • Pavement replacement (1 lane)	• Inspection/tests (08:00–20:00, Weekday 2): 2 lanes closed in busiest carriageway for 2 days • Partial bridge repair (08:00–20:00, Weekday 2): 2 lanes closed for 3 days • Central safety barrier replacement (22:00–06:00, Weekday 2): travel + overtaking lanes closed in both directions for 1 night; traffic on emergency lane • Pavement replacement (20:00–23:00, Weekday 2): travel + overtaking lanes closed for 3 h
7	• Lost toll revenue: fire brigade (17:00–18:00, Weekday 1): full carriageway closed for 1 h • Bridge demolition • Bridge reconstruction • Bridge load test • Lost toll revenue, 3 nights (demolition, launching, load test, 22:00–06:00, Weekday 2) • Noise barriers • Lateral safety barriers • Pavement replacement (1 lane)	• Reconstruction works (08:00–20:00): 1 lane closed per day for 6 consecutive days (2× Weekday 1, 3× Weekday 2, 1× Holiday); 3 days southbound, 3 days northbound • Noise barrier replacement: only emergency lane closed • Lateral barrier replacement (20:00–23:00, Weekday 2): emergency + travel lane for 3 h • Pavement replacement (20:00–23:00, Weekday 2): emergency + travel lane for 3 h
8	• Lost toll revenue: fire brigade (17:00–19:00, Weekday 1): full carriageway closed for 2 h • Bridge demolition • Bridge reconstruction • Bridge load test • Lost toll revenue: 3 nights (demolition, launching, load test, 22:00–06:00, Weekday 2) • Central median barrier • Full pavement replacement (entire carriageway)	• Reconstruction works (08:00–20:00): 1 lane closed per day for 6 consecutive days (2× Weekday 1, 3× Weekday 2, 1× Holiday); 3 days southbound, 3 days northbound • Central safety barrier replacement (22:00–06:00, Weekday 2): travel + overtaking lanes closed for 1 night; traffic on emergency lane • Full pavement replacement (22:00–03:00, Weekday 2): entire carriageway closed for 5 h; traffic diverted to opposite carriageway

Table 9
Impacts of the eight heavy vehicle fire scenarios analysed regarding the arch bridge.

Scenario	Estimated Direct Costs	Estimated Indirect Costs
1	None	None, one lane (emergency or travel lane) closed for fire brigade; remaining two lanes kept open.
2	• Noise barriers • Lateral safety barriers	• Fire brigade (17:00–18:00, Weekday 1): emergency + travel lane closed for 1 h • Noise barrier replacement: only emergency lane closed • Lateral barrier replacement (20:00–23:00, Weekday 2): emergency + travel lane closed for 3 h
3	• Central median barrier • Lost toll revenue: full carriageway closed for 1 h (17:00–18:00, Weekday 1)	• Central safety barrier replacement (22:00–06:00, Weekday 2): travel + overtaking lanes closed in both directions for 1 night; traffic on emergency lane
4	None	None, one lane (emergency or travel lane) closed for fire brigade; remaining two lanes kept open.
5	• Structural inspection & tests • Bridge load test • Lost toll revenue (load test, 22:00–06:00, Weekday 2): both carriageways closed for 1 night • Partial bridge repair (7.5% of construction cost — half of girder bridge value) • Noise barriers • Lateral safety barriers • Pavement replacement (1 lane)	• Fire brigade (17:00–18:00, Weekday 1): emergency + travel lane closed for 1 h • Inspection/tests (08:00–20:00, Weekday 2): 2 lanes closed in busiest carriageway for 2 days • Partial bridge repair (08:00–20:00, Weekday 2): 2 lanes closed for 1 day • Noise barrier replacement: only emergency lane closed • Lateral barrier replacement (20:00–23:00, Weekday 2): emergency + travel lane for 3 h • Pavement replacement (20:00–23:00, Weekday 2): emergency + travel lane for 3 h
6	• Lost toll revenue: fire brigade (17:00–18:00, Weekday 1): full carriageway closed for 1 h • Structural inspection & tests • Bridge load test • Lost toll revenue (load test, 22:00–06:00, Weekday 2): both carriageways closed for 1 night • Partial bridge repair (10% of construction cost) • Central median barrier • Pavement replacement (1 lane)	• Inspection/tests (08:00–20:00, Weekday 2): 2 lanes closed in busiest carriageway for 2 days • Partial bridge repair (08:00–20:00, Weekday 2): 2 lanes closed for 2 days • Median barrier replacement (22:00–06:00, Weekday 2): travel + overtaking lanes closed in both directions for 1 night; traffic on emergency lane • Pavement replacement (20:00–23:00, Weekday 2): travel + overtaking lanes closed for 3 h
7	• Structural inspection & tests • Bridge load test • Lost toll revenue (load test, 22:00–06:00, Weekday 2): both carriageways closed for 1 night • Partial bridge repair (40% of construction cost) • Noise barriers • Lateral safety barriers • Pavement replacement (1 lane)	• Fire brigade (17:00–18:00, Weekday 1): emergency + travel lane closed for 1 h • Inspection/tests (08:00–20:00, Weekday 2): 2 lanes closed in busiest carriageway for 2 days • Partial bridge repair (08:00–20:00): 1 lane closed for 6 consecutive days (2× Weekday 1, 3× Weekday 2, 1× Holiday); 3 days southbound, 3 days northbound • Noise barrier replacement: only emergency lane closed • Lateral barrier replacement (20:00–23:00, Weekday 2): emergency + travel lane for 3 h • Pavement replacement (20:00–23:00, Weekday 2): emergency + travel lane for 3 h
8	• Lost toll revenue: fire brigade (17:00–19:00, Weekday 1): full carriageway closed for 2 h • Structural inspection & tests • Bridge load test • Lost toll revenue (load test, 22:00–06:00, Weekday 2): both carriageways closed for 1 night • Partial bridge repair (50% of construction cost) • Central median barrier • Pavement replacement (1 lane)	• Inspection/tests (08:00–20:00, Weekday 2): 2 lanes closed in busiest carriageway for 2 days • Partial bridge repair (08:00–20:00): 1 lane closed for 8 consecutive days (2× Weekday 1, 3× Weekday 2, 2× Holiday); 4 days southbound, 4 days northbound • Median barrier replacement (22:00–06:00, Weekday 2): travel + overtaking lanes closed for 1 night; traffic on emergency lane • Pavement replacement (20:00–23:00, Weekday 2): travel + overtaking lanes closed for 3 h

Table 10
Estimated financial costs related to the girder and arch overpass (Indicative values for the methodology demonstration).

Description	Girder overpass		Arch overpass	
	Estimated financial cost [€]	Normalization	Estimated financial cost [€]	Normalization
Construction of the overpass	3,100,000.00 €	-	4,500,000.00 €	-
Demolition of the overpass	240,000.00 €	8%	N/A	N/A
Inspection and structural test	1500.00 €	0.05%	1500.00 €	0.03%
Bridge load testing	5000.00 €	0.16%	5000.00 €	0.11%
Replacement of components damaged by lateral fire position (heavy vehicles – moderate fire intensity)	465,000.00 €	15%	232,500.00 €	5%
Replacement of components damaged by central fire position (heavy vehicles – moderate fire intensity)	620,000.00 €	20%	310,000.00 €	7%
Replacement of components damaged by lateral fire position (heavy vehicles – Severe fire intensity)	N/A (Collapse)	N/A (Collapse)	1,800,000.00 €	40%
Replacement of components damaged by central fire position (heavy vehicles – Severe fire intensity)	N/A (Collapse)	N/A (Collapse)	2,250,000.00 €	50%

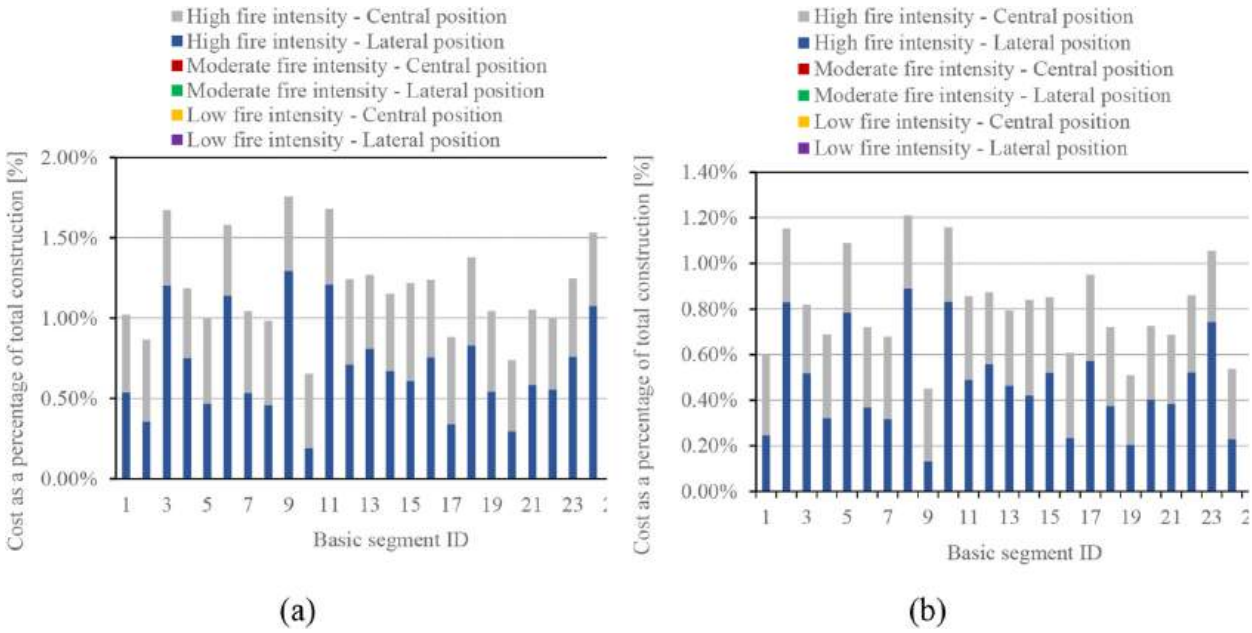


Fig. 12. Costs as percentage of total construction due to light vehicles fires: (a) girder overpass; (b) arch bridge.

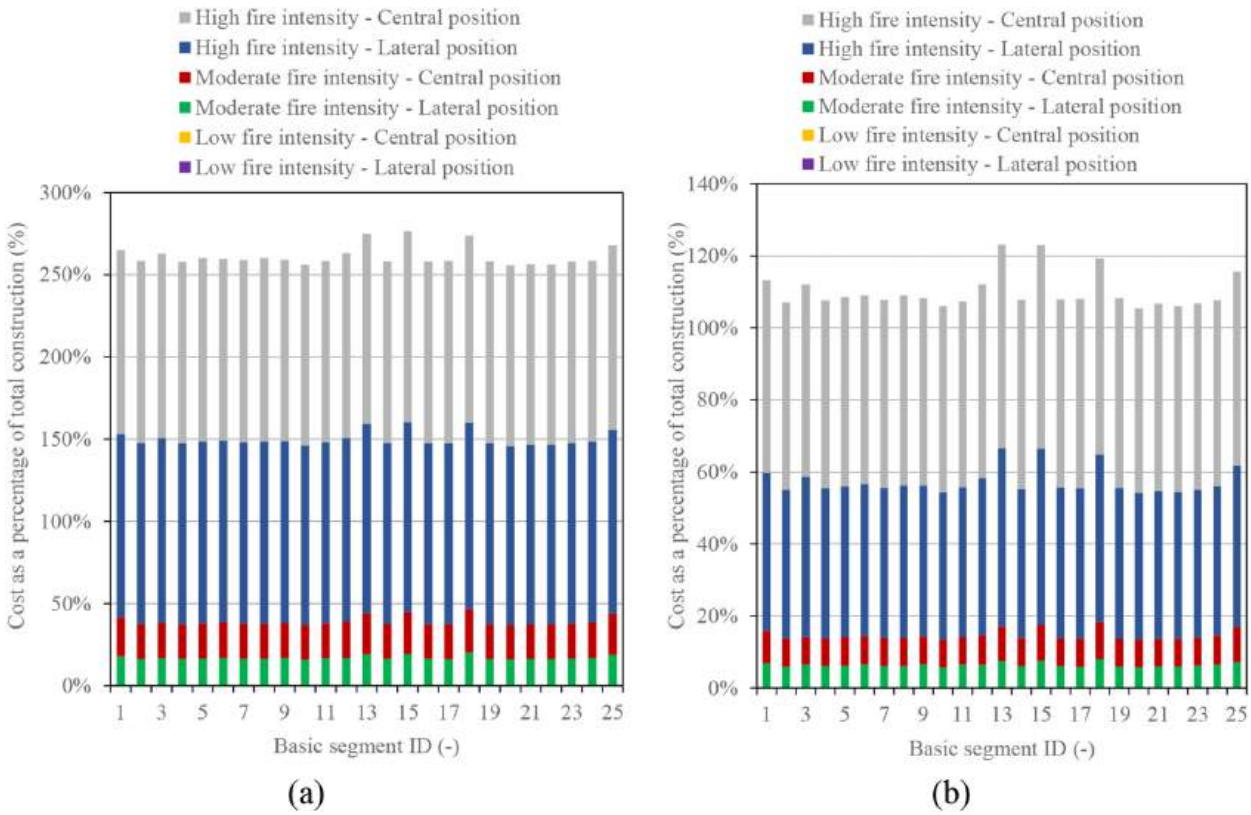


Fig. 13. Costs as percentage of total construction due to heavy vehicles fires: (a) girder overpass; (b) arch bridge.

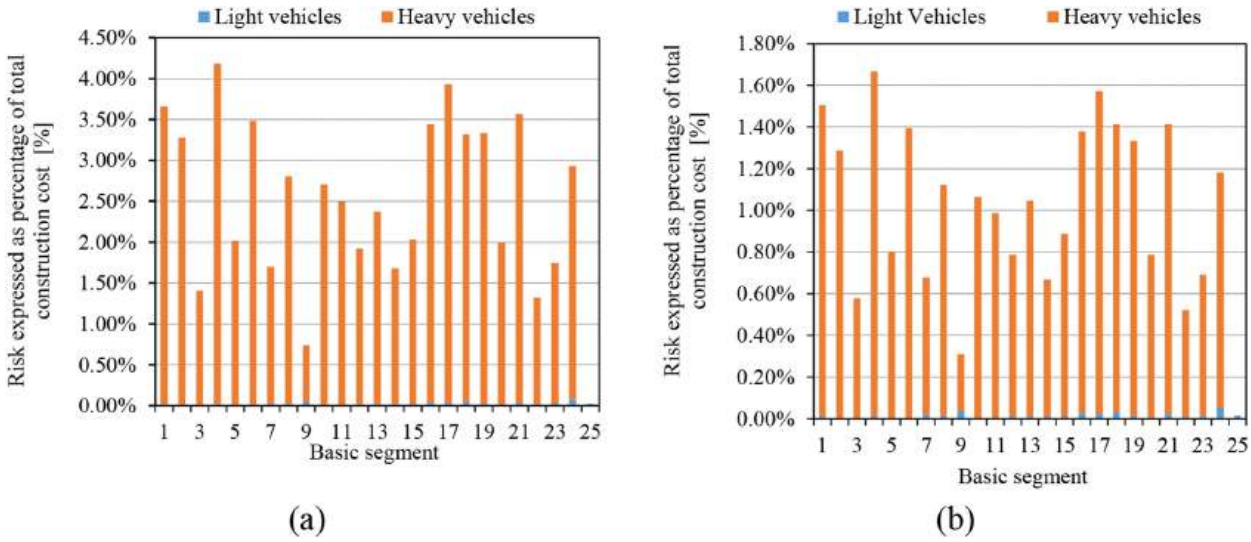


Fig. 14. Risk expressed as percentage of total estimated construction cost: (a) girder overpass; (b) arch bridge.

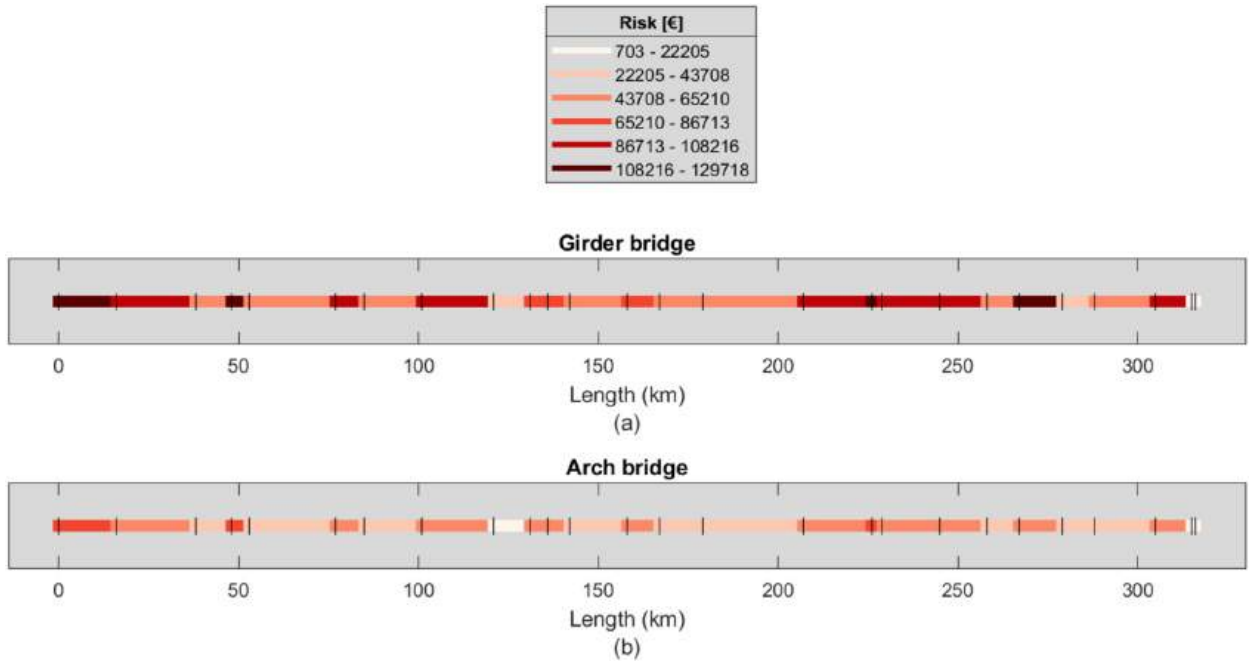


Fig. 15. a) risk associated with a girder bridge; b) risk associated with an arch bridge.

consequences of a fire are assumed to change as follows.

- in the absence of intumescent paint, a fire with moderate damage to the heavy vehicle would cause partial damage to the bridge, while a fire with severe damage to the heavy vehicle would cause the collapse of a girder bridge and severe damage to an arch bridge;
- in the presence of intumescent paint, a fire with moderate damage to the heavy vehicle is assumed to cause no damage to the bridge, while a fire with severe damage to the heavy vehicle causes only partial damage (15% of the construction cost for the girder bridge with fire in a lateral position and 20% for a fire in a central position. For the arch bridge, half of these values are assumed). Furthermore, it is expected that both types of fires will require reapplication of the intumescent paint. It is assumed that this operation is performed during the night hours, with the closure of both lanes of the motorway, thus generating direct costs due to the missed revenue tolls.

Table 11
Risk Associated in the basic segment.

Basic Segment n°	N° of Overpasses	Girder bridge	Arch bridge	Risk Associated in the basic segment [€]
1	2	1	1	181,259
2	3	2	1	261,115
3	5	4	1	200,862
4	1	0	1	75,011
5	1	0	1	36,054
6	4	3	1	386,995
7	7	6	1	346,467
8	11	10	1	919,765
9	6	5	1	128,618
10	1	0	1	47,910
11	2	1	1	121,835
12	6	5	1	332,699
13	8	7	1	562,051
14	1	0	1	30,097
15	17	16	1	1,046,860
16	10	9	1	1,022,469
17	2	1	1	192,570
18	12	11	1	1,195,238
19	12	11	1	1,196,314
20	6	5	1	345,342
21	7	6	1	726,574
22	5	4	1	187,407
23	11	10	1	571,334
24	9	8	1	778,969
25	1	0	1	703
			Total [€]	**10,894,518**

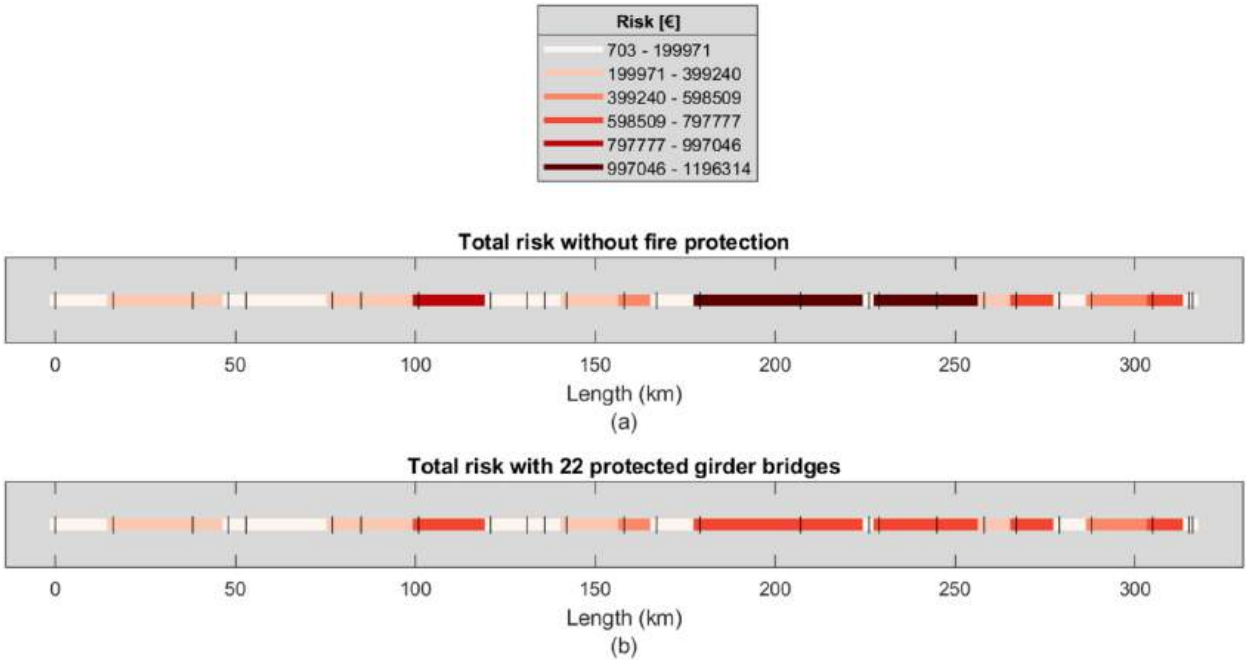


Fig. 16. Comparison of risk without fire protection (a) and risk with twenty-two protected girder bridges with intumescent paint (b).

After having found that the protection of arch bridges does not offer significant benefits, the assumption of applying fire protection to girder bridges was analysed, in particular, to five bridges in the basic segments 15, 18 and 19, to four bridges in section 16, to two in section 8 and to one in section 24. The investment to protect twenty-two girder bridges is € 6,245,525.34.

Fig. 16 illustrates the risk related to each motorway's basic section for the girder and arch bridge, highlighting the components related to light and heavy vehicles. These results refer to the overpasses present in each basic segment and the with and without intumescent paint protection.

However, it is essential to emphasise that the calculated risk represents an underestimate of the actual risk, as it does not account for the costs associated with users crossing above the overpass. Following a fire event on an overpass, these users would face a prolonged closure lasting months or even years, forcing them to use alternative routes and thereby increasing travel times and transportation costs. As previously mentioned, this indirect cost component is difficult to quantify and was therefore not included in the present study. Although the protection of these bridges may be of lesser interest to the infrastructure operator, since such bridges connect local or regional roads rather than the highway directly, the indirect costs associated with the users travelling over the bridge are extremely high because they accumulate over an extended period. This aspect could be of particular interest to the municipalities or provinces affected by the closure, which might therefore decide to contribute to the initial investment. The selection of the overpasses to be protected should therefore be guided by the average daily traffic crossing each bridge. A high traffic volume indicates that the bridge plays a particularly important role within the local transportation network and should consequently be considered a priority for protection measures.

6. Conclusions

This study presented a risk-based framework for assessing fire hazard in highway bridges, applied to an important European motorway as a real-world case study. The methodology integrates the Highway Safety Manual's predictive approach with structural consequence analysis and cost estimation for bridge fire accidents, enabling a quantitative assessment of fire risk at the network level. The application to the analysed motorway demonstrated that fire risk varies significantly across the motorway segments, with the highest risk concentrated in segments with dense heavy-vehicle traffic and multiple overpasses. The structural typology plays a critical role: given that the fire scenarios are located under the bridge and do not significantly affect the structural capacity of the arch, girder bridges with composite steel-concrete sections are substantially more vulnerable, exhibiting collapse under severe fire scenarios below the overpasses. The cost analysis revealed that indirect costs, primarily travel time losses due to lane closures, often exceed direct repair costs, underscoring the economic importance of rapid and targeted intervention. The application of intumescent paint as a fire protection measure was shown to reduce risk significantly for the most exposed girder bridges, with an estimated investment of approximately €6.2 million yielding a total risk reduction of several million euros across the 22 most critical overpasses. These findings demonstrate that the proposed Bridge Management System can serve as a practical decision-support tool for infrastructure managers, enabling risk-informed prioritisation of fire protection investments.

In future research, it would be necessary to implement a methodology to incorporate the costs borne by users travelling across the bridge itself, which were not included in the present study due to the inherent difficulty of quantification. Given that a fire-induced closure of an overpass may last several months or even years, the associated indirect costs, in terms of increased travel time and distance for diverted users, could be substantial and would provide a complete and more accurate estimate of the true fire risk. Future work could also be extended to other bridge typologies and, with appropriate adaptations, to contexts where individual fire events may be less frequent but potentially more catastrophic in terms of the number of people involved and the nature of hazardous materials transported, such as railway bridges.

CRediT authorship contribution statement

Patrick Covi: Writing – review & editing, Writing – original draft, Visualization, Validation, Methodology, Investigation, Formal analysis, Data curation, Conceptualization. **Marco Guerrieri:** Writing – review & editing, Writing – original draft, Validation, Supervision, Methodology, Investigation, Conceptualization. **Nicola Tondini:** Writing – review & editing, Writing – original draft, Supervision, Methodology, Conceptualization.

Declaration of competing interest

The authors declare that they have no known competing financial interests or personal relationships that could have appeared to influence the work reported in this paper.

Acknowledgements

This research has been supported by Fondazione CARITRO Cassa di Risparmio di Trento e Rovereto for the “FIREBRIDGE” project (grant number 2022.0228).

The consortium RELUIS (DM 204 1/07/2022) is acknowledged, and the authors also acknowledge the Italian Ministry of Education, Universities and Research (MUR), in the framework of the project DICAM-EXC (Departments of Excellence 2023-2027, grant L232/2016).

Appendix

Table A. 1
CMFs for highways.

CMF	CMF description	Equation
$CMF_{1,fs\ ac\ y\ z}$	presence of planimetric curves	$CMF_{1,fs\ ac\ y\ z} = 1 + a \cdot \left[\sum_{i=1}^{m} \left(\frac{5.730}{R_i}\right)^2 \cdot P_{c,i}\right]$ Where: - $CMF_{1,\ fs,\ ac,\ y,\ z}$: Crash modification factor for horizontal curvature in a freeway segment with any cross-section ac; - m = number of horizontal curves in the segment; - Ri* = equivalent radius of curve i (=$[0.5/R_{a,i}^2 + 0.5/R_{b,i}^{2]-0.5}$ if both roadbeds are curved, $R_{a,i}$ if only one roadbed is curved) (ft); - $R_{a,i}$ = radius of curve i in one roadbed (ft); - $R_{b,i}$ = radius of curve i in second roadbed (used if both roadbeds are curved) (ft); and - $P_{c,\ i}$ = proportion of effective segment length with curve i.
$CMF_{2,w,x,y,fi}$	crash modification factor for lane width	$CMF_{2,y,fi} = \begin{cases} \exp(a \cdot [W_l\text{-}12]) & \text{if } W_l < 13 \text{ ft} \\ b \text{ if} & W_l \geq 13 \text{ ft} \end{cases}$ Where: - W_l = lane width (ft)
$CMF_{3,w,x,y,z}$	crash modification factor for inside shoulder width	$CMF_{3,y,z} = \exp(a \cdot [W_{is}\text{-}6])$ Where: - W_{is} = paved inside shoulder width (ft).
$CMF_{4,w,x,y,z}$	crash modification factor for median width	$CMF_{4,y,z} = (1\text{-}P_{ib}) \cdot \exp(a \cdot [W_m\text{-}2W_{is}\text{-}48]) + P_{ib} \cdot \exp(a \cdot [2W_{icb}\text{-}48])$ Where: - P_{ib} = proportion of effective segment length with a barrier present in the median (i.e., inside); - W_m = median width (measured from near edges of travelled way in both directions) (ft); and - W_{icb} = distance from edge of inside shoulder to barrier face (ft).
$CMF_{5,w,x,y,z}$	crash modification factor for median barrier	$CMF_{5,y,z} = (1\text{-}P_{ib}) + P_{ib} \cdot \exp\left(\frac{a}{W_{icb}}\right)$ Where: - P_{ib} = proportion of effective segment length with a barrier present in the median (i.e., inside); - W_{icb} = distance from edge of inside shoulder to barrier face (ft).
$CMF_{6,w,x,y,z}$	crash modification factor for high volume	$CMF_{6,y,z} = \exp(a \cdot P_{hv})$ Where: P_{hv} = proportion of AADT during hours where volume exceeds 1000 veh/h/ln.
$CMF_{7,fs,ac,mv,z}$	crash modification factor for lane changes	$CMF_{7,mv,z} = 1$ (the base condition is no significant lane changing due to ramp entry or exit).
$CMF_{8,fs,ac,sv,z}$	crash modification factor for outside shoulder width	$CMF_{8,sv,z} = \left(1\text{-}\sum_{i=1}^{m} P_{c,i}\right) \cdot \exp(a \cdot [W_s\text{-}10]) + \left(\sum_{i=1}^{m} P_{c,i}\right) \cdot \exp(b \cdot [W_s\text{-}10])$ Where: - W_s = paved outside shoulder width (ft).
$CMF_{9,fs,ac,sv,fi}$	crash modification factor for shoulder rumble strips	$CMF_{9,sv,fi} = 1$ (The base condition is no shoulder rumble strips present)
$CMF_{10,fs,ac,sv,fi}$	crash modification factor for outside clearance	$CMF_{10,sv,fi} = (1\text{-}P_{ob}) \cdot \exp(\text{-}0.00451 \cdot [W_{hc}\text{-}W_s\text{-}20]) + P_{ob} \cdot \exp(\text{-}0.00451 \cdot [W_{ocb}\text{-}20])$ Where: - P_{ob} = proportion of effective segment length with a barrier present on the roadside (i.e., outside); - W_{hc} = clear zone width (ft); and - W_{ocb} = distance from edge of outside shoulder to barrier face (ft).
$CMF_{11,fs,ac,sv,z}$	crash modification factor for roadside barrier	$CMF_{11,sv,z} = (1\text{-}P_{ob}) + P_{ob} \cdot \exp\left(\frac{a}{W_{ocb}}\right)$ Where: - W_{ocb} and P_{ob} are described before

* The values of the coefficients a and b are provided in the HSM.

Table A. 2
Expected mean accident frequencies under basic conditions for all vehicle types.

Basic Segment n°	**AADT_eq** [**veh** /**day**]	$\mathbf{N_{spf,mv,fi}}/\mathbf{L}^*$ $\left[\frac{\text{crashes}}{\text{km} \cdot \text{year}}\right]$	$\mathbf{N_{spf,sv,fi}}/\mathbf{L}^*$ $\left[\frac{\text{crashes}}{\mathbf{km} \cdot \mathbf{year}}\right]$	$\mathbf{N_{spf,mv,pdo}}/\mathbf{L}^*$ $\left[\frac{\text{crashes}}{\mathbf{km} \cdot \mathbf{year}}\right]$	$\mathbf{N_{spf,sv,pdo}}/\mathbf{L}^*$ $\left[\frac{\text{crashes}}{\mathbf{km} \cdot \mathbf{year}}\right]$
1	42848	0.4289	0.8381	0.9202	1.7837
2	45839	0.4743	0.8755	1.0486	1.8923
3	50861	0.5539	0.9363	1.2824	2.0727
4	49055	0.5248	0.9147	1.1957	2.0081
5	52740	0.5847	0.9585	1.3757	2.1396
6	51265	0.5604	0.9411	1.3021	2.0871

(*continued on next page*)

Table A. 2 (*continued*)

Basic Segment n°	**AADT_eq** [**veh** /**day**]	$\mathbf{N_{spf,mv,fi}/L^*}$ $\left[\frac{\text{crashes}}{\text{km} \cdot \text{year}}\right]$	$\mathbf{N_{spf,sv,fi}/L^*}$ $\left[\frac{\text{crashes}}{\mathbf{km} \cdot \mathbf{year}}\right]$	$\mathbf{N_{spf,mv,pdo}/L^*}$ $\left[\frac{\text{crashes}}{\mathbf{km} \cdot \mathbf{year}}\right]$	$\mathbf{N_{spf,sv,pdo}/L^*}$ $\left[\frac{\text{crashes}}{\mathbf{km} \cdot \mathbf{year}}\right]$
7	60955	0.7256	1.0524	1.8206	2.4289
8	61837	0.7414	1.0623	1.8720	2.4597
9	61051	0.7273	1.0535	1.8262	2.4323
10	55195	0.6257	0.9871	1.5023	2.2266
11	53605	0.5990	0.9686	1.4197	2.1703
12	62119	0.7464	1.0654	1.8885	2.4695
13	63058	0.7633	1.0758	1.9442	2.5022
14	64764	0.7943	1.0945	2.0473	2.5614
15	65275	0.8037	1.1000	2.0787	2.5791
16	50726	0.5517	0.9347	1.2758	2.0679
17	63546	0.7721	1.0811	1.9734	2.5191
18	66003	0.8171	1.1079	2.1238	2.6042
19	64367	0.7871	1.0901	2.0231	2.5476
20	64291	0.7857	1.0893	2.0185	2.5450
21	64661	0.7924	1.0933	2.0410	2.5578
22	57618	0.6672	1.0149	1.6326	2.3120
23	58367	0.6801	1.0234	1.6740	2.3383
24	62876	0.7600	1.0737	1.9334	2.4958
25	64018	0.7807	1.0863	2.0019	2.5355

Table A. 3
Expected mean accident frequencies under basic conditions for light vehicle.

Basic Segment n°	light vehicles [%]	$\mathbf{N_{spf,mv,fi}/L^*}$ $\left[\frac{\text{crashes}}{\text{km} \cdot \text{year}}\right]$	$\mathbf{N_{spf,sv,fi}/L^*}$ $\left[\frac{\text{crashes}}{\text{km} \cdot \text{year}}\right]$	$\mathbf{N_{spf,mv,pdo}/L^*}$ $\left[\frac{\text{crashes}}{\text{km} \cdot \text{year}}\right]$	$\mathbf{N_{spf,sv,pdo}/L^*}$ $\left[\frac{\text{crashes}}{\text{km} \cdot \text{year}}\right]$
1	44%	0.1873	0.3660	0.4018	0.7789
2	45%	0.2134	0.3939	0.4718	0.8514
3	45%	0.2497	0.4221	0.5782	0.9345
4	45%	0.2377	0.4143	0.5416	0.9096
5	47%	0.2736	0.4486	0.6438	1.0014
6	46%	0.2552	0.4286	0.5930	0.9505
7	48%	0.3511	0.5092	0.8808	1.1751
8	49%	0.3616	0.5181	0.9130	1.1996
9	49%	0.3559	0.5156	0.8937	1.1903
10	50%	0.3098	0.4887	0.7439	1.1025
11	51%	0.3082	0.4983	0.7303	1.1165
12	54%	0.4042	0.5769	1.0227	1.3373
13	52%	0.3940	0.5553	1.0036	1.2916
14	51%	0.4070	0.5608	1.0490	1.3124
15	51%	0.4111	0.5627	1.0634	1.3193
16	56%	0.3103	0.5256	0.7175	1.1629
17	56%	0.4312	0.6037	1.1020	1.4067
18	51%	0.4175	0.5662	1.0853	1.3308
19	52%	0.4072	0.5640	1.0467	1.3181
20	51%	0.3965	0.5497	1.0187	1.2844
21	50%	0.3968	0.5475	1.0221	1.2808
22	51%	0.3368	0.5124	0.8243	1.1673
23	50%	0.3427	0.5157	0.8435	1.1783
24	52%	0.3933	0.5557	1.0006	1.2917
25	51%	0.4006	0.5574	1.0271	1.3009

Table A. 4
Expected mean accident frequencies under basic conditions for heavy vehicle.

Basic Segment n°	heavy vehicles [%]	$\mathbf{N_{spf,mv,fi}/L^*}$ $\left[\frac{\text{crashes}}{\text{km} \cdot \text{year}}\right]$	$\mathbf{N_{spf,sv,fi}/L^*}$ $\left[\frac{\text{crashes}}{\text{km} \cdot \text{year}}\right]$	$\mathbf{N_{spf,mv,pdo}/L^*}$ $\left[\frac{\text{crashes}}{\text{km} \cdot \text{year}}\right]$	$\mathbf{N_{spf,sv,pdo}/L^*}$ $\left[\frac{\text{crashes}}{\text{km} \cdot \text{year}}\right]$
1	56%	0.2414	0.4718	0.5180	1.0041
2	55%	0.2607	0.4813	0.5764	1.0403
3	55%	0.3040	0.5139	0.7038	1.1376
4	55%	0.2869	0.5001	0.6537	1.0979
5	53%	0.3109	0.5096	0.7314	1.1376
6	54%	0.3050	0.5122	0.7088	1.1360
7	52%	0.3744	0.5430	0.9394	1.2532

(*continued on next page*)

Table A. 4 (*continued*)

Basic Segment n°	heavy vehicles [%]	$N_{spf,mv,fi}/L^*$ $\left[\frac{crashes}{km \cdot year}\right]$	$N_{spf,sv,fi}/L^*$ $\left[\frac{crashes}{km \cdot year}\right]$	$N_{spf,mv,pdo}/L^*$ $\left[\frac{crashes}{km \cdot year}\right]$	$N_{spf,sv,pdo}/L^*$ $\left[\frac{crashes}{km \cdot year}\right]$
8	51%	0.3796	0.5439	0.9585	1.2595
9	51%	0.3712	0.5377	0.9320	1.2413
10	50%	0.3158	0.4981	0.7581	1.1236
11	49%	0.2907	0.4701	0.6890	1.0534
12	46%	0.3421	0.4882	0.8655	1.1317
13	48%	0.3692	0.5203	0.9403	1.2101
14	49%	0.3872	0.5335	0.9980	1.2485
15	49%	0.3924	0.5371	1.0150	1.2593
16	44%	0.2413	0.4088	0.5580	0.9045
17	44%	0.3408	0.4772	0.8711	1.1120
18	49%	0.3994	0.5416	1.0382	1.2730
19	48%	0.3785	0.5242	0.9728	1.2250
20	49%	0.3878	0.5377	0.9963	1.2561
21	50%	0.3942	0.5439	1.0154	1.2725
22	49%	0.3290	0.5005	0.8051	1.1402
23	50%	0.3361	0.5057	0.8272	1.1555
24	48%	0.3653	0.5161	0.9293	1.1997
25	49%	0.3788	0.5270	0.9713	1.2301

Table A. 5
Values of the Crash Modification Factors (CMFs) for each basic segment of the analysed motorway.

Basic Segment N°	1	2	3	4	5	6	7	8	9	10	11	12	13	14	15	16	17	18	19	20	21	22	23	24	25
$CMF_{1,mv,fi}$	1.09	1.07	1.05	1.05	1.13	1.08	1.01	1.01	1.01	1.01	1.01	1.01	1.02	1.03	1.02	1.01	1.01	1.00	1.00	1.00	1.01	1.00	1.00	1.00	1.00
$CMF_{1,mv,pdo}$	1.17	1.14	1.10	1.11	1.26	1.17	1.02	1.02	1.02	1.03	1.03	1.03	1.04	1.06ì	1.03	1.02	1.02	1.01	1.01	1.00	1.01	1.01	1.00	1.01	1.00
$CMF_{1,sv,fi}$	1.36	1.29	1.21	1.23	1.55	1.36	1.04	1.04	1.04	1.06	1.06	1.06	1.08	1.13	1.06	1.04	1.04	1.01	1.01	1.01	1.03	1.02	1.01	1.01	1.01
$CMF_{1,sv,pdo}$	1.32	1.25	1.19	1.20	1.48	1.32	1.03	1.03	1.03	1.05	1.05	1.06	1.08	1.11	1.05	1.04	1.03	1.01	1.01	1.01	1.03	1.01	1.01	1.01	1.01
$CMF_{2,y,fi}$	0.99	0.99	0.99	0.99	0.99	0.99	0.99	0.99	0.99	0.99	0.99	0.99	0.99	0.99	0.99	0.99	0.99	0.99	0.99	0.99	0.99	0.99	0.989	0.99	0.99
$CMF_{3,y,fi}$	1.09	1.09	1.09	1.09	1.09	1.09	1.09	1.09	1.09	1.09	1.09	1.09	1.09	1.09	1.09	1.09	1.09	1.09	1.09	1.09	1.09	1.09	1.09	1.09	1.09
$CMF_{3,y,pdo}$	1.08	1.08	1.08	1.08	1.08	1.08	1.08	1.08	1.08	1.08	1.08	1.08	1.08	1.08	1.08	1.08	1.08	1.08	1.08	1.08	1.08	1.08	1.08	1.08	1.08
$CMF_{4,mv,fi}$	1.15	1.15	1.15	1.15	1.15	1.15	1.15	1.15	1.15	1.15	1.15	1.15	1.15	1.15	1.15	1.15	1.15	1.06	1.06	1.06	1.06	1.06	1.06	1.06	1.06
$CMF_{4,mv,pdo}$	1.14	1.14	1.14	1.14	1.14	1.14	1.14	1.14	1.14	1.14	1.14	1.14	1.14	1.14	1.14	1.14	1.14	1.06	1.06	1.06	1.06	1.06	1.06	1.06	1.06
$CMF_{4,sv,fi}$	1.05	1.05	1.048	1.05	1.05	1.05	1.05	1.048	1.05	1.05	1.05	1.05	1.05	1.05	1.05	1.05	1.05	1.02	1.02	1.02	1.02	1.02	1.02	1.02	1.02
$CMF_{4,sv,pdo}$	1.14	1.14	1.14	1.14	1.14	1.14	1.14	1.14	1.14	1.14	1.14	1.14	1.14	1.14	1.14	1.14	1.14	1.06	1.06	1.06	1.06	1.06	1.06	1.06	1.06
$CMF_{5,y,fi}$	1.17	1.17	1.17	1.17	1.17	1.17	1.17	1.17	1.17	1.17	1.17	1.17	1.17	1.17	1.17	1.17	1.17	1.01	1.01	1.01	1.01	1.01	1.01	1.01	1.01
$CMF_{5,y,pdo}$	1.22	1.22	1.22	1.22	1.22	1.22	1.22	1.22	1.22	1.22	1.22	1.22	1.22	1.22	1.22	1.22	1.22	1.01	1.01	1.01	1.01	1.01	1.01	1.01	1.01
$CMF_{6,mv,fi}$	1.01	1.01	1.01	1.01	1.01	1.01	1.01	1.01	1.01	1.01	1.01	1.01	1.01	1.01	1.01	1.01	1.01	1.01	1.01	1.01	1.01	1.01	1.01	1.01	1.01
$CMF_{6,mv,pdo}$	1.01	1.01	1.01	1.01	1.01	1.01	1.01	1.01	1.01	1.01	1.01	1.01	1.01	1.01	1.01	1.01	1.01	1.01	1.01	1.01	1.01	1.01	1.01	1.01	1.01
$CMF_{6,sv,fi}$	0.99	0.99	0.99	0.99	0.99	0.99	0.9	0.99	0.99	0.99	0.99	0.99	0.99	0.99	0.99	0.99	0.99	0.99	0.99	0.99	0.99	0.99	0.99	0.99	0.99
$CMF_{6,sv,pdo}$	0.97	0.97	0.97	0.97	0.97	0.97	0.97	0.97	0.97	0.97	0.97	0.97	0.97	0.97	0.97	0.97	0.97	0.97	0.97	0.97	0.97	0.97	0.97	0.97	0.97
$CMF_{7,mv,fi}$	1.00	1.00	1.00	1.00	1.00	1.00	1.00	1.00	1.00	1.00	1.00	1.00	1.00	1.00	1.00	1.00	1.00	1.00	1.00	1.00	1.00	1.00	1.00	1.00	1.00
$CMF_{7,mv,pdo}$	1.00	1.00	1.00	1.00	1.00	1.00	1.00	1.00	1.00	1.00	1.00	1.00	1.00	1.00	1.00	1.00	1.00	1.00	1.00	1.00	1.00	1.00	1.00	1.00	1.00
$CMF_{8,sv,fi}$	1.15	1.14	1.15	1.15	1.23	1.25	1.14	0.89	0.89	0.89	1.03	0.89	0.89	0.89	0.89	0.89	1.14	1.14	1.13	1.13	1.14	1.13	1.14	1.14	1.12
$CMF_{8,sv,pdo}$	1.10	1.07	1.08	1.09	1.18	1.15	1.07	0.95	0.96	0.94	1.02	0.94	0.93	0.93	0.93	0.94	1.05	1.05	1.03	1.04	1.06	1.04	1.05	1.06	1.01
$CMF_{9,sv,fi}$	1.00	1.00	1.00	1.00	1.00	1.00	1.00	1.00	1.00	1.00	1.00	1.00	1.00	1.00	1.00	1.00	1.00	1.00	1.00	1.00	1.00	1.00	1.00	1.00	1.00
$CMF_{10,sv,fi}$	1.09	1.09	1.09	1.09	1.09	1.09	1.09	1.09	1.09	1.09	1.09	1.09	1.09	1.09	1.09	1.09	1.09	1.09	1.09	1.09	1.09	1.09	1.09	1.09	1.09
$CMF_{11,sv,fi}$	1.14	1.14	1.14	1.14	1.14	1.14	1.14	1.14	1.14	1.14	1.14	1.14	1.14	1.14	1.14	1.14	1.14	1.14	1.14	1.14	1.14	1.14	1.14	1.14	1.14
$CMF_{11,sv,pdo}$	1.18	1.18	1.18	1.18	1.18	1.18	1.18	1.18	1.18	1.18	1.18	1.18	1.18	1.18	1.18	1.18	1.18	1.18	1.18	1.18	1.18	1.18	1.18	1.18	1.18

Data availability

The data that has been used is confidential.

References

[1] V. Kodur, M.Z. Naser, Fire hazard in transportation infrastructure: review, assessment, and mitigation strategies, Front. Struct. Civ. Eng. 15 (2021) 46–60, https://doi.org/10.1007/s11709-020-0676-6.

[2] J. Hu, R. Carvel, A. Usmani, Bridge fires in the 21st century: a literature review, Fire Saf. J. 126 (2021) 103487, https://doi.org/10.1016/j.firesaf.2021.103487.

[3] Redazione Cronaca, Strage in A21, la perizia non lascia scampo: il cavalcavia è da abbattere. Corriere della *Sera* [in Italian], https://brescia.corriere.it/notizie/cronaca/18_gennaio_31/strage-a21-perizia-cavalcavia-brescia-cremona-abbattere-339afc8a-0660-11e8-8b64-d2626c604009.shtml, 2018, January 31.

[4] BresciaToday, Montirone-poncarale, cavalcavia A21. BresciaToday. https://www.bresciatoday.it/motori/news/montirone-poncarale-cavalcavia-a21.html, 2018 [in Italian].

[5] B. Raspa, Montirone, nuovo ponte: via ai lavori, Il Giorno (2018, December 6). https://www.ilgiorno.it/brescia/cronaca/montirone-ponte-fecf5bb8 [in Italian].

[6] L. Deng, W. Wang, Y. Yu, State-of-the-art review on the causes and mechanisms of bridge collapse, J. Perform. Constr. Facil. 30 (2) (2016) 04015005, https://doi.org/10.1061/(ASCE)CF.1943-5509.0000731.
[7] E.E.M. Diaz, F.N. Moreno, J. Mohammadi, Investigation of common causes of bridge collapse in Colombia, Pract. Period. Struct. Des. Construct. 14 (4) (2009) 194–200, https://doi.org/10.1061/(ASCE)SC.1943-5576.0000006.
[8] G.C. Lee, S. Mohan, C. Huang, B.N. Fard, A Study of US Bridge Failures (1980-2012), MCEER, Buffalo, NY, 2013.
[9] J. Scheer, Failed Bridges: Case Studies, Causes and Consequences, John Wiley & Sons, 2011.
[10] J. Alos-Moya, I. Paya-Zaforteza, A. Hospitaler, E. Loma-Ossorio, Valencia bridge fire tests: validation of simplified and advanced numerical approaches to model bridge fire scenarios, Adv. Eng. Software 128 (2019) 55–68, https://doi.org/10.1016/j.advengsoft.2018.11.003.
[11] E. Aziz, V. Kodur, An approach for evaluating the residual strength of fire exposed bridge girders, J. Constr. Steel Res. 88 (2013) 34–42, https://doi.org/10.1016/j.jcsr.2013.04.007.
[12] J.C. Dotreppe, S. Majkut, J.M. Franssen, Failure of a tied-arch bridge submitted to a severe localized fire, in: IABSE Symposium Lisbon, 2005.
[13] I. Payá-Zaforteza, M.E. Garlock, A numerical investigation on the fire response of a steel girder bridge, J. Constr. Steel Res. 75 (2012) 93–103, https://doi.org/10.1016/j.jcsr.2012.03.012.
[14] C. Song, G. Zhang, V. Kodur, Y. Zhang, S. He, Fire response of horizontally curved continuous composite bridge girders, J. Constr. Steel Res. 182 (2021) 106671, https://doi.org/10.1016/j.jcsr.2021.106671.
[15] G. Zhang, C. Song, X. Li, S. He, Q. Huang, Fire performance of continuous steel-concrete composite bridge girders, KSCE J. Civ. Eng. 25 (3) (2021) 973–984, https://doi.org/10.1007/s12205-021-0985-x.
[16] J. Alos-Moya, I. Paya-Zaforteza, A. Hospitaler, P. Rinaudo, Valencia bridge fire tests: experimental study of a composite bridge under fire, J. Constr. Steel Res. 138 (2017) 538–554, https://doi.org/10.1016/j.jcsr.2017.08.008.
[17] I. Kaundinya, U. Bergerhausen, J. Schmidt, Effects of extreme fire scenarios on bridges, Bridge Struct. 13 (4) (2018) 159–167, https://doi.org/10.3233/BRS-170117.
[18] M. Garlock, I. Paya-Zaforteza, V. Kodur, L. Gu, Fire hazard in bridges: review, assessment and repair strategies, Eng. Struct. 35 (2012) 89–98, https://doi.org/10.1016/j.engstruct.2011.11.002.
[19] P. Covi, N. Tondini, Numerical investigation of a steel tied arch bridge under fire loading, ce/papers 6 (3–4) (2023) 2086–2091, https://doi.org/10.1002/cepa.2517.
[20] P. Covi, N. Tondini, Probabilistic fire assessment of bridges: an Italian case study. SIF 2024 Conference, Coimbra, 2024.
[21] A. Abarca, R. Monteiro, G.J. O'Reilly, Simplified methodology for indirect loss–based prioritisation in roadway bridge network risk assessment, Int. J. Disaster Risk Reduct. 74 (2022) 102948, https://doi.org/10.1016/j.ijdrr.2022.102948.
[22] World Health Organization, Global Status Report on Road Safety 2023: Country and Territory Profiles, World Health Organization, 2024.
[23] Istat road accidents – 2023, available: 2024, https://www.istat.it/en/.
[24] H.M. Al-Ahmadi, A. Jamal, T. Ahmed, M.T. Rahman, I. Reza, D. Farooq, Calibrating the highway safety manual predictive models for multilane rural highway segments in Saudi Arabia, Arabian J. Sci. Eng. 46 (11) (2021) 11471–11485, https://doi.org/10.1007/s13369-021-05944-6.
[25] E. DeNicola, O.S. Aburizaize, A. Siddique, H. Khwaja, D.O. Carpenter, Road traffic injury as a major public health issue in the Kingdom of Saudi Arabia: a review, Front. Public Health 4 (2016) 215, https://doi.org/10.3389/fpubh.2016.00215.
[26] National Research Council (US). Transportation research board. Task force on development of the highway safety manual, & transportation officials. Joint task force on the highway safety manual. (2010). "Highway safety manual (Vol. 1)". AASHTO.
[27] F. La Torre, L. Domenichini, V. Branzi, M. Meocci, A. Paliotto, N. Tanzi, Transferability of the highway safety manual freeway model to EU countries, Accid. Anal. Prev. 178 (2022) 106852, https://doi.org/10.1016/j.aap.2022.106852.
[28] I.C. Matarage, S. Dissanayake, Quality assessment between calibrated highway safety manual safety performance functions and calibration functions for predicting crashes on freeway facilities, J. Traffic Transport. Eng. 7 (1) (2020) 76–87, https://doi.org/10.1016/j.jtte.2019.12.001.
[29] B. Claros, C. Sun, P. Edara, HSM calibration factor, calibration function, or jurisdiction-specific safety model-A comparative analysis, J. Transport. Saf. Secur. 12 (2) (2020) 309–328, https://doi.org/10.1080/19439962.2018.1477896.
[30] P. Alluri, D. Saha, A. Gan, Minimum sample sizes for estimating reliable highway safety manual (HSM) calibration factors, J. Transport. Saf. Secur. 8 (1) (2016) 56–74, https://doi.org/10.1080/19439962.2014.978963.
[31] O.B.B. Mendes, A.P.C. Larocca, K. Rodrigues Silva, A. Pirdavani, "Assessing the performance of highway safety manual (HSM)". Predictive models for Brazilian multilane highways, Sustainability 15 (13) (2023) 10474, https://doi.org/10.3390/su151310474.
[32] S. Dadvar, Y.J. Lee, H.S. Shin, Improving crash predictability of the highway safety manual through optimizing local calibration process, Accid. Anal. Prev. 136 (2020) 105393, https://doi.org/10.1016/j.aap.2019.105393.
[33] Regulation (EU) N. 1316/2013 of the European Parliament and of the Council of 11 December 2013, stablishing the Connecting Europe Facility, Amending Regulation (EU) No 913/2010 and Repealing Regulations (EC) No 680/2007 and (EC) No 67/2010.
[34] AASHTO, Highway Safety Manual (HSM), Chapter 18 - Predictive Method for Freeways, American Association of State Highway Transportation Officials (AASHTO), 2014.
[35] HCM (Highway Capacity Manual), A Guide for Multimodal Mobility Analysis, seventh ed., Transportation Research Board, National Academies Press, 2022.
[36] GCBA, Guide to Cost-Benefit Analysis of Investment Projects, European commission, 2014, https://doi.org/10.2776/97516.
[37] Ministero delle Infrastrutture e dei Trasporti, Linee guida per la valutazione degli investimenti in opere pubbliche [Guidelines for the evaluation of investments in public works], Rome, Italy, 2017 [in Italian].
[38] EN 1993-1-2, Eurocode 3: Design of Steel Structures - Part 1-2: General Rules - Structural Fire Design, 2005.
[39] J.B. Schleich, L.G. Cajot, M. Pierre, M. Brasseur, J.M. Franssen, D. Joyeux, G. Aurtenetxe, Development of Design Rules for Steel Structures Subjected to Natural Fires in Closed Car Parks, CEC, 1999.
[40] C. Fraud, B. Zhao, D. Joyeux, J. Kruppa, Guide Pour la Vérification du Comportement au Feu de Parcs de Stationnement Large Mentventilés en Superstructure Métallique, CTICM, INSI–03/233d–BZ/PB (2004) 75.
[41] M.J. Hurley, D.T. Gottuk, J.R. Hall Jr, K. Harada, E.D. Kuligowski, M. Puchovsky, C.J. Wieczorek (Eds.), SFPE Handbook of Fire Protection Engineering, Springer, 2015.
[42] D. De Silva, M. Gallo, L. De Falco, E. Nigro, Fire risk assessment of bridges: from state of the art to structural vulnerability mitigation, Journal of Civil Structural Health Monitoring 13 (8) (2023) 1613–1632, https://doi.org/10.1007/s13349-023-00670-z.
[43] Autonomous Province of Bolzano - South Tyrol, Fire Service, "Current Interventions." Official website (Accessed online, 3 October 2026).
[44] Polizia di Stato (Italian State Police), Official Website. Official Website (Accessed online, 3 October 2026).
[45] County of Los Angeles fire department, Official Website. Official Website (Accessed online, 3 October 2026).
[46] Marion County Fire Rescue, Marion County, Florida, Official Website. Official Website (Accessed online, 3 October 2026).
[47] Queensland Fire Department, Official Website. Official Website (Accessed online, 3 October 2026).
[48] P. Covi, F. Di Meglio, D. de Silva, A. Miano, E. Nigro, N. Tondini, Fire fragility functions of bridges subjected to vehicle fire scenarios. SIF 2026 Conference, Kingston, Canada, 2026.